EBioMedicine 44 (2019) 261–274

Contents lists available at ScienceDirect

EBioMedicine

journal homepage: www.ebiomedicine.com

EBioMedicine
Published by THE LANCET

Research paper

CCAAT/enhancer binding protein delta (C/EBPδ) demonstrates a dichotomous role in tumour initiation and promotion of epithelial carcinoma

Ramlogan Sowamber [a,b], Rania Chehade [a,b], Mahmoud Bitar [a,b], Leah V. Dodds [e,g], Anca Milea [a,b], Brian Slomovitz [e,f,g], Patricia A. Shaw [a,b,c,d], Sophia H.L. George [e,f,g,*]

[a] Campbell Family Institute for Breast Cancer Research, Toronto, Ontario, Canada
[b] Princess Margaret Cancer Center, University Health Network, Toronto, Ontario, Canada
[c] Department of Laboratory Medicine and Pathobiology, Toronto, Ontario, Canada
[d] University of Toronto, Toronto, Ontario, Canada
[e] Sylvester Comprehensive Cancer Center, Miami, Florida, United States
[f] Department of Obstetrics and Gynecology and Reproductive Sciences, Division of Gynecology Oncology, Miami, Florida, United States
[g] University of Miami, Leonard Miller School of Medicine, Miami, Florida, United States

ARTICLE INFO

Article history:
Received 26 February 2019
Received in revised form 1 May 2019
Accepted 2 May 2019
Available online 9 May 2019

Keywords:
C/EBPδ
High-grade serous ovarian cancer
Fallopian tube epithelia
Epithelial to mesenchymal transition

ABSTRACT

Background: CCAAT/enhancer binding protein delta (C/EBPδ,*CEBPD*), a gene part of the highly conserved basic-leucine zipper (b-ZIP) domain of transcriptional factors, is downregulated in 65% of high grade serous carcinomas of the ovary (HGSC). Overexpression of C/EBPδ in different tumours, such as glioblastoma and breast cancer either promotes tumour progression or inhibits growth and has low expression in normal tissue until activated by cytotoxic stressors.

Methods: Higher overall expression of C/EBPδ in the luteal phase of the menstrual cycle prompted us to investigate the role of C/EBPδ in carcinogenesis. In vitro experiments were conducted in fallopian tube cell samples and cancer cell lines to investigate the role of C/EBPδ in proliferation, migration, and the epithelial to mesenchymal transition.

Findings: Expression of C/EBPδ induced premature cellular arrest and decreased soft agar colony formation. Loss of C/EBPδ in epithelial cancer cell lines did not have significant effects on proliferation, yet overexpression demonstrated downregulation of growth, similar to normal fallopian tube cells. C/EBPδ promoted a partial mesenchymal to epithelial (MET) phenotype by upregulating E-cadherin and downregulating Vimentin and N-cadherin in FTE cells and increased migratory activity, which suggests a regulatory role in the epithelial-mesenchymal plasticity of these cells.

Interpretation: Our findings suggest that C/EBPδ regulates the phenotype of normal fallopian tube cells by acting on downstream regulatory factors that are implicated in the development of ovarian serous carcinogenesis.

Fund: This study was funded by the CDMRP Ovarian Cancer program (W81WH-0701-0371, W81XWH-18-1-0072), the Princess Margaret Cancer Centre Foundation, Foundation for Women's Cancer – The Belinda-Sue/Mary-Jane Walker Fund, Colleen's Dream Foundation and Sylvester Comprehensive Cancer Center.

1. Introduction

High-grade serous ovarian cancer (HGSC) remains the most fatal gynecological malignancy and accounts for the majority of deaths due to ovarian cancer [1,2]. Improving early detection, prevention and overall prognosis was limited by a lack of understanding of the etiology of HGSC. Now, significant data suggests the distal end of the fallopian tube is the site of origin for HGSC [3]. Detailed histopathological examination of the fallopian tube epithelium in *BRCA* mutation carriers undergoing prophylactic bilateral salpingo-oophorectomy led to the identification of precursor lesions [4–6].

A pre-neoplastic lesion called the p53 signature is the earliest mutational and genomic event described in the gradual steps of HGSC development [7]. The acquisition of somatic *TP53* mutations is followed by

* Corresponding author at: Department of Obstetrics, Gynecology, and Reproductive Sciences, Division of Gynecologic Oncology, Sylvester Comprehensive Cancer Center, Leonard Miller School of Medicine, University of Miami, 1550 NW 10th Ave, Pap Building, Room 403 (M-877), Miami, FL 33136, United States.
E-mail address: sophia.george@med.miami.edu (S.H.L. George).

https://doi.org/10.1016/j.ebiom.2019.05.002

Research in context

Evidence before this study

High Grade Serous Carcinoma is the fifth most lethal gynecological malignancy with poor overall survival rates. Early detection is paramount to reducing the lethality of the disease in later stages of carcinogenesis. Despite numerous advances in the field, the etiology of the disease and its development and origin from the Fallopian tube remains not fully understood. Our previous work suggested that C/EBPδ responds to inflammation and acute cytotoxic stresses induced by ovulation in BRCA1 mutation carriers. Moreover, C/EBPδ has been shown to be a tumour suppressor in breast cancers, but a master regulator and oncogene in glioblastoma multiforme. Its function therefore is context dependent and no studies currently have determined its role in the initiation of ovarian cancer.

Added value of this study

This study sheds light on the role of C/EBPδ in normal Fallopian tube epithelia and cancer. We show that C/EBPδ decreases cell growth and promotes a mesenchymal to epithelial transition in epithelial cells. Using in vitro assays, we show that C/EBPδ also increases the migration potential of these cells, demonstrating a dichotomous role for C/EBPδ. Together, this data show that C/EBPδ is capable of modulating downstream factors which can alter the phenotype of the cells and regulate the development of the disease.

Implications of all the available evidence

Our research indicates that C/EBPδ is an important transcriptional regulator in the initiation of ovarian cancer from the Fallopian tubes. C/EBPδ enables cells to maintain an epithelial-like phenotype and decreases proliferation in normal cells. In cancer cells, C/EBPδ promotes migration, EMT/MET, cell survival through IL-6/STAT3 signals and promotes genomic stability. In toto, evidence suggests that C/EBPδ could be an attractive target for therapy in certain cancer types.

additional genomic alterations, cellular tufting, and loss of polarity, resulting in the development of neoplastic serous tubal intraepithelial carcinoma (STIC) [8–14]. STIC lesions share multiple genomic copy number alterations, along with mutations in tumour suppressors and oncogenes, including *TP53*, *BRCA1* and *BRCA2*, *RB1*, *STK11*, *FOXO3a*, *CCNE1*, *STATHMIN1*, and *hTERT*, which are observed prior to HGSC metastasis to the ovaries and peritoneal spread [8,12,15–23]. In this model, cells that exfoliate from the fallopian tube into the peritoneal cavity must evade anoikis and detachment associated apoptosis before attaching to the mesothelial ovarian surface [24,25].

The fallopian tube epithelia (FTE) undergo monthly cycles of hormonally driven proliferation and differentiation. In a previous study, we identified CCAAT/enhancer binding protein delta (C/EBPδ, *CEBPD*), to be transcriptionally upregulated in the FTE of *BRCA1* mutation carriers and in the post-ovulatory (luteal) phase of the ovarian cycle, a process linked to cytotoxic stress [26]. *C/EBPδ* is located on chromosome 8q11.21 and belongs to the superfamily of highly conserved basic-leucine zipper (b-ZIP) domain transcriptional factors [27]. It has multiple functions related to inflammation, cell cycle regulation, differentiation, and metabolism [26–29]. Although C/EBPδ overexpression promotes glioblastoma progression and is associated with poor progression in pancreatic and urothelial cancers [30,31], its overexpression in breast, prostate, and myeloid cancers, inhibits growth and promotes differentiation [32–34]. Furthermore, low expression of C/EBPδ was reported in cervical, hepatocellular carcinoma [35,36], breast [37], prostate cancer [38], and leukemia [32]. C/EBPδ's pro-oncogenic/tumour suppressive function is cell type and context dependent [30,35,39–41]. Little is known about the role of C/EBPδ in the development of HGSC. The objectives of this study were to explore expression of C/EBPδ in HGSC tumours as well as precursor lesions and determine the effects of C/EBPδ on FTE cancer cell growth and migration.

2. Material and methods

2.1. Case collection

The University Health Network Research Ethics Board approved the study protocol for collection of tissue and clinical information for all patients. Each patient provided written informed consent allowing for the collection and use of tissue for research purposes. H&E sections of high-grade serous carcinoma, borderline and low-grade serous carcinoma were reviewed by a gynecological pathologist (P.S.) prior to use in the study. Diagnosis of each case was retrieved from the UHN ovarian tissue bank prior to review. To validate immunohistochemical protein expression of samples, whole sections of tissue were cut from formalin fixed paraffin embedded tissue and analyzed as in our previous publication [8,15,42]. A previously published cohort ($n = 15$) of serous tubal intraepithelial carcinoma (STIC) cases using Abcam morphological and immunohistological features including cellular crowding, loss of nuclear polarity and presence of p53 and Ki67, from women having adnexal high-grade serous carcinoma [8,15,43].

2.2. Immunohistochemistry

Immunohistochemistry was performed using standard procedures as previously described [44] with the following modifications. The following antibodies were used at these dilutions: Ki67 (Lab Vision, Thermo Scientific, Waltham, Massachusetts, USA) 1/1000; p53 (Novocastra, Leica, Wetzlar, Germany) 1/200; C/EBPδ 1/200 (sc-636) (Santa Cruz Biotechnology, Inc., Dallas, Texas, USA); E-cadherin 1/100 (AB15148) (Abcam, Cambridge, United Kingdom); Vimentin 1/100 (5741S) (Cell Signaling Technology, Danvers, Massachusetts, USA). Appropriate negative and positive controls were performed to determine specificity of antibodies. Stained slides were scanned using the ScanScope XT slide scanner (Aperio Technologies, Inc., Leica) to create digital images at 40× magnification which were then quantified for intensity and percentage of cells staining using a nuclear algorithm as previously described (Spectrum Plus, Image Analysis Toolbox, TMALab II, Aperio, Inc.) [26,42]. Intensity levels were based on an absorption range scale of 0 to 255 (0 = black; 255 = white). Weak Intensity Staining (1+) ranged from 200 to 215; medium intensity staining (2+) from 180 to 200; and strong intensity staining (3+) from 0 to 180. Intensity levels +2 and + 3 were combined to create a composite score for the percent positive nuclei present in each case. Images were annotated to include only epithelium while excluding stroma.

2.3. Immunofluorescence

Cells were grown in 6-well plates (Falcon) coated with collagen IV and fixed with 4% PFA for 5 min, permeabilized with 0.3% Triton-X/PBS then blocked with 5% goat serum (Gibco, Life technologies) in PBS. Primary antibodies: C/EBPδ (SC-636), CK18 (M701029) (Dako, Agilent Technologies, Santa Clara, California, United States), Pax8 (10336-1-AP) (ProteinTech, Rosemont, IL, USA), E-cadherin (AB15148) (Abcam), Vimentin (5741S) (Cell Signaling), were applied overnight at 4 °C. Primary antibody was removed by washing samples with 1× PBS three times and was incubated with appropriate fluorophore-labeled secondary antibodies (Jackson ImmunoResearch

Laboratories, West Grove, PA, USA) and Vectashield (H-1200, Vector Laboratories, Burlingame, CA, USA) in a dark area for 45 min. Cells were again washed for three times with 1× PBS and was mounted onto a coverslip and dried in the dark for 10 min. Samples were visualized using a Leica Axioimager (Leica).

2.4. Fallopian tube epithelia tissue cultures

Surgical samples were obtained from the University Health Network with patient consent and Research Board Ethics Approval. In brief, fimbriae were collected after prophylactic hysterectomy or salpingo-oophorectomy and incubated for 4-16 h at 37 °C in pronase and subsequently cultured as previously described [8]. Three independent patient derived fallopian tubes were used in this study: 71-FTE, age 50; 57-FTE, age 29; and 19-FTE, age 48. Cells were immortalized via infection with a lentiviral dominant negative TP53 (R175H) vector and retroviruses human telomerase (hTERT) [8]. Cells were infected with a lenti-viral C/EBPδ overexpression construct 24-48 h after cells reached 70% confluence. Each plate was grown till 70% confluence and harvested for different molecular assays. For biological replicates, all molecular analyses of cell lines for RNA and protein extraction were performed from the cell population. That is, at time of collection, cells were divided into two pellets. Additionally, for FACS and immunofluorescence, the same population of cells were pelleted for RNA and protein assays.

2.5. Cell lines

SKOV3, OVCAR3, MCF7, MDA231, T47D were obtained from the ATCC (Manassa, Virginia, USA). SKOV3 (ATCC-HBT-77) was grown in McCOY's 5a (Life technologies, Carlsbad, California, USA) supplemented with 10% fetal bovine serum (FBS, Wisent technologies, St-Bruno, Quebec

Canada). MCF7 (ATCC-HTB-22) and MDA231 (ATCC-HTB-26) cells were grown in DMEM/F12 (Life technologies), supplemented with 10% FBS. T47D (ATCC-HTB-133) and OVCAR3 (HTB-161) cells were grown in RPMI-1640 (Life technologies), supplemented with 10% and 20% FBS, respectively. Culture method was followed as described by ATCC for each cell line. Kuramochi (JCRB No. JCRB0098) and OVSAHO (JCRB No. JCRB1046) cells were obtained from JCRB (Japanese Collection of Research Bioresources) Cell Bank and Sekisui Xenotech LLC (Cambridge, Kansas City, USA). Cells were grown in RPMI-1640 (Life technologies) supplemented with 10% FBS.

2.6. Virus production and infection

HEK-293T cells were seeded at a density of 1.0 × 10^6 cells per plate in a 6 cm tissue culture dish overnight with low antibiotic growth media (DMEM +10% FBS). Cells were incubated until 70% confluence was achieved. A mixture of three transfection plasmids were produced by combining 2 μg pMDG.2 (Addgene #12259) (Addgene, Watertown, Massachusetts, USA); 4 μg of pCMV delta R8.2 (Addgene #12263) and 5 μg of vector (pCDH-CMV-MCS-EF1-GFP empty, pCDH-CMV-MCS-EF1-GFP-C/EBPδ - C/EBPδ-OE). As per manufacturer's protocol, GenJet DNA In-vitro Transfection reagent (Ver. II) (SignaGen Laboratories, Rockville, MD, USA) was used as the transfection reagent. Reagents were added to each plate drop-wise and was incubated overnight (16 h, 37 °C, 5% CO_2). Next day, media was subsequently removed and replaced with high BSA growth media and again incubated for 24 h. Supernatant was then collected and passed through a 0.45 μm filter and snap frozen and stored at −80 °C until required for use. A second round of collection was performed 72 h after virus transfection and was also filtered and stored at −80 °C.

2.7. Protein isolation, western blot and antibodies

Cell samples were washed with 1× PBS and trypsinized using 0.25% trypsin dissociation reagent (Life technologies) for 5 min at 37 °C. Trypsin neutralizing solution (TNS) was added to samples and was spun at 1000 rpm for 5 min. Supernatant was aspirated, and samples were placed on ice before lysing. Cells were lysed with NP40 buffer (Life technologies) and protease inhibitor cocktail (Thermo Scientific). Samples were incubated for 15 min on ice and subsequently clarified by centrifugation (14,000 rpm for 30 min). The supernatant was collected and quantified using BioRad DC Protein Assay (BioRad Laboratories, Hercules, California, United States). Samples were re-suspended in 4× LDS sample buffer (Life technologies), boiled, and 30 μg of protein was resolved by SDS-Page 4–12% Bis-tris Gels (Novex, Life technologies). Protein samples were transferred to BioRad PVDF membrane and were blocked with 5% milk powder dissolved in 1× TBS-T for 1 h or overnight. Primary antibodies were diluted in blocking buffer (5% skimmed milk, Nestle, Vevey, Switzerland) and incubated with membranes overnight at 4 °C. Membranes were washed for 10 min, three times and probed with secondary antibody, washed three times for 15 min using 1× TBS-T, and developed using ECL Prime western blotting detection reagent (GE Healthcare Life Sciences, Pittsburgh, PA, USA). Each membrane was imaged using BioRad ChemiDoc and images analyzed using BioRad Image Lab software (BioRad ImageLab v5.2.1, build 11). The following antibodies were used in western blots: C/EBPδ (Santa Cruz, SC-636, 1/200) (In some instances, this polyclonal antibody has produced double bands as seen in Fig. 4d), B-actin (Sigma, A2228, 1/1000) (Sigma-Aldrich, St. Louis, Missouri, USA), P53 (Santa Cruz; sc-126, 1/500), PAX8 (ProteinTech, 10,336-1-AP, 1/1000), Snail (Cell Signaling, 3895S, 1/500), Slug (Cell Signaling, 9585S, 1/500) Vimentin (Cell Signaling, 5741S, 1/500), E-cadherin (Abcam, AB15148 1/500), E-cadherin (Cell Signaling, 24E10,#3195, 1/500), N-cadherin (SantaCruz, sc-7939, 1/500), SIP1 (Santa Cruz, sc-48,789, 1/200), Twist (Santa cruz, sc-81,417, 1/500), and goat HRP-IgG (anti-mouse or anti-rabbit) (Santa Cruz, 1:10,000). Western Blot quantification for C/EBPδ protein was carried out across each cell line using ImageLab imaging software (BioRad ImageLab, v5.2.1, build 11)(Supplementary Figs. S2e and S5d). Raw values, measured in units of intensity (INT) were used to graph protein expression.

2.8. Cloning strategy

Overexpression vectors were constructed using pCDH-CMV-MCS-EF1-GFP cloning/expression vector (System Biosciences, Palo Alto, CA, USA). C/EBPδ insert was cut out of a PCR4 TOPO cloning vector (Invitrogen, Carlsbad, California, USA) using *Eco*RI (New England Biolabs (NEB), Ipswich, Massachusetts, USA). The cDNA was then ligated into pCDH-CMV-MCS-EF1-GFP using Takara ligation Kit (Clontech, Mountain View, California, USA) and was confirmed in the expression vector by DNA sequencing at The Centre for Applied Genomics (SickKids, Toronto, Ontario, Canada). Lentivirus was produced using HEK-293 T cells (Clontech) and the overexpression vector was confirmed in the cells by GFP fluorescence and western blot (Fig. 2a-b, Supplementary Fig. S4a).

2.9. Fluorescence activated cell sorting (FACS)

For cell cycle regulation assessment, cells were washed in 1× PBS and 10 μM BrdU-APC was added to cells in a dark environment. Plates with BrdU were then incubated at 37 °C for 4 h. Cells were then washed twice with ice cold PBS, trypsinized with 0.25% trypsin dissociation reagent and neutralized for counting. Nuclei preparation and staining was performed by adding 0.08% Pepsin and 2 N HCl and IFA/0.5%, Tween20 (Sigma). Samples were incubated in the dark and 100 μl anti-BrdU-APC was added while samples were incubated on ice. 5 μg/ml of propidium iodide (PI) was added to cells and incubated on ice

for 15 min. Flow cytometry was carried out on BD FACS Calibur (BD biosciences, San Jose, CA, USA). Data was analyzed using FlowJo v10 (Flowjo LLC, Ashland, OR, USA). Cell surface staining was performed on single cell suspension. EpCAM-PE (Life technologies, VU-1D9) and CD49f-APC (FAB13501A) (R&D Biosystems, Minneapolis, Minnesota, USA) was added to the cell suspension and incubated in the dark for 40-60 min. Cells were then washed and centrifuged at 400 *g* for 5 min at room temperature and subsequently vortexed to dissociate pellet. Stained cells were re-suspended in staining buffer and flow cytometry performed on BD Calibur flow cytometer (BD biosciences).

2.10. Soft agar assay

Base agar (1% agarose Difco Agar Noble, BD biosciences) was added to 6-well plates and allowed to solidify for 5 min. Top agarose layer was made by combining 0.7% agarose with media. 5000 cells were added to the mixture and plated on 6-well plate. Cells were kept in an incubator at 37 °C for 14 days. Cells were fed twice a week. After 14 days, each plate well was stained with 0.5 ml of crystal violet (0.005%) for approximately 1 h. Plates were then imaged using a dissecting microscope and camera setup (Leica). Images were imported into ImageJ (v1.47), National Institute of Health, Bethesda, Maryland, USA) and analyzed in GraphPad (GraphPad, La Jolla California USA, Version 8.0.1 (244) using an unpaired *t*-test ($p < 0.05$).

2.11. Quantitative PCR

RNA was isolated from FTE cells lysed with Trizol reagent (Invitrogen). 1 μg of total RNA was reverse-transcribed using qScript cDNA SuperMix (Quanta Biosciences, Beverly, MA, USA). Real-time quantitative PCR (RT-qPCR) was performed using PerfeCTa Sybr Green FastMix, Rox (Quanta Biosciences) according to the manufacturer's protocol using the ABI PRISM 7900HT Sequence Detection System (Applied Biosystems, Foster City, California, USA). The target CT values were normalized to b-actin. The N-fold differential expression was assessed using the $2^{-(\Delta\Delta CT)}$ method to determine differences between treated cells and controls. Primer sequences were obtained from PrimerBank [45,46]. qRT-PCR as mean ± SEM. An unpaired *t*-test with $n = 3$, $p \leq 0.05$ was determined in GraphPad Image Analysis Software, unless noted otherwise in text. $N = 3$ represents 3 independent experiments with 3 technical replicates within each experiment.

2.12. miRNA assay

FTE cells were harvested from 6 cm plates and RNA was isolated using miRNAeasy micro kit (Qiagen, Hilden, Germany). Quantity and quality of total RNA was analyzed using Nanodrop (Thermo Scientific). RNA was reverse transcribed into cDNA using miScript II RT kit (Qiagen). cDNA was then processed using miScript SYBR Green PCR kit (Qiagen) and was run on miScript miRNA PCR Array Human Ovarian Cancer plates (Qiagen, MIHS-110ZE-4, 384-well plate). PCR plates were read on the ABI PRISM 7900HT Sequence Detection System (Applied Biosystems). Results were outputted with $2^{-\Delta Ct}$ values for each gene in each treatment group compared to the control group (n = 3). Qiagen software was used to analyze results and student's *t*-test provided statistically significant miRNA ($p < 0.05$).

2.13. Wound-healing assay

63857 p53DN-hTERT (57-FTE), 3619 p53DN-hTERT (19-FTE) cells were seeded in 96-well plates (Essen ImageLock) and grown to confluence. Scratch wounds were generated using the 96-pin WoundMaker (Essen BioScience, Ann Arbor, MI, USA) and wells were gently washed with 1× PBS to remove non-adherent cells. Cells were imaged using the INCUCYTE™ Kinetic Imaging System (Essen BioScience) and wound width (μm) was determined using the INCUCYTE™ cell migration software module.

2.14. Migration assay

MCF7 cells and FTE cells were seeded onto Costar Transwell migration assay (Corning Costar 3472) (Corning Inc., Corning, New York, USA) at a density of 50,000 cells. Plated cells were initially grown in serum free media for 24 h. After trypsinization using Trypsin (EDTA 0.25%) (Life Technologies), cells were counted and plated onto the Transwell migration assay which was then placed in DMEM/F12 + 10% FBS for 12 h. Transwell's were then removed from the assay and washed with PBS and H_2O to remove unbound cells. 1% Crystal Violet +2% ethanol was added to the Transwell and allowed to incubate at room temperature for 15 min at which point the wells were rinsed with H_2O and dried. Each well was imaged using an inverted microscope (Leica) and cells were counted in ImageJ (ImageJ labs). Results were analyzed with an unpaired *t*-test ($p < 0.05$) and graphed using GraphPad graphing software (GraphPad, La Jolla California USA, Version 8.0.1 (244)).

2.15. Proliferation assay

For a proliferation assay, 3.0×10^4 cells were seeded onto a 6-well plate (Falcon, Corning Inc.) and plated with 2 ml of fresh media. Cells were counted every 1–3 days using CyQuant Direct Proliferation Assay kit (Life technologies). An inverted plate reader (Flexstation 3) (Molecular Devices, San Jose, California, USA) was used to quantify the amount of fluorescence emitted by live cells and provide a count of live cells present. Softmax Pro software (Molecular Devices) was to measure fluorescence and results were analyzed using an unpaired *t*-test in GraphPad ($p < 0.05$).

2.16. Statistical analysis

Statistical analysis was performed using GraphPad Prism Software (GraphPad, Version 8.0.1 (244)). The Log-rank test was used in Kaplan-Meier, Mantel-Cox regression analysis to compare *C/EBPδ* expression on overall survival and progression free survival. MicroRNA analysis was performed using Qiagen SaBiosciences miScript miRNA PCR Array Data Analysis Software (Qiagen, v1.1). Values are expressed as means ± SEM and were experiments were performed three times. Unpaired *t*-tests were performed to determine statistical significance, unless otherwise noted. A value with $p < 0.05$ was considered to be statistically significant.

3. Results

3.1. C/EBPδ protein expression across two distinct histoypes (low grade serous and high grade serous tumours) varies

We previously reported higher expression levels of C/EBPδ at the mRNA and protein levels in the luteal phase of the normal fallopian tube epithelia [26]. To investigate C/EBPδ protein expression levels across serous ovarian cancer histotypes, immunohistochemistry was performed on a cohort of 366 high grade serous carcinoma (HGSC) and 26 low-grade serous carcinoma (LGSC) on five independent tissue microarrays (TMAs). The C/EBPδ protein is localized primarily to the nucleus of the cell with some diffuse cytoplasmic staining. Each core was annotated to include epithelia and exclude stroma. Mean intensity and percent positivity using a nuclear stain algorithm was reported based on the following histoscores: no expression (0); low (+1); medium (+2), and high (+3) (Fig. 1a). In FTE, C/EBPδ protein is expressed in the nuclei of secretory and ciliated cells. Seventy-six per cent (76.5%, 280/366) of HGSC cases had low or attenuated (histoscore of 0/+1) C/EBPδ protein expression whereas 24% (86/366) had a medium to high

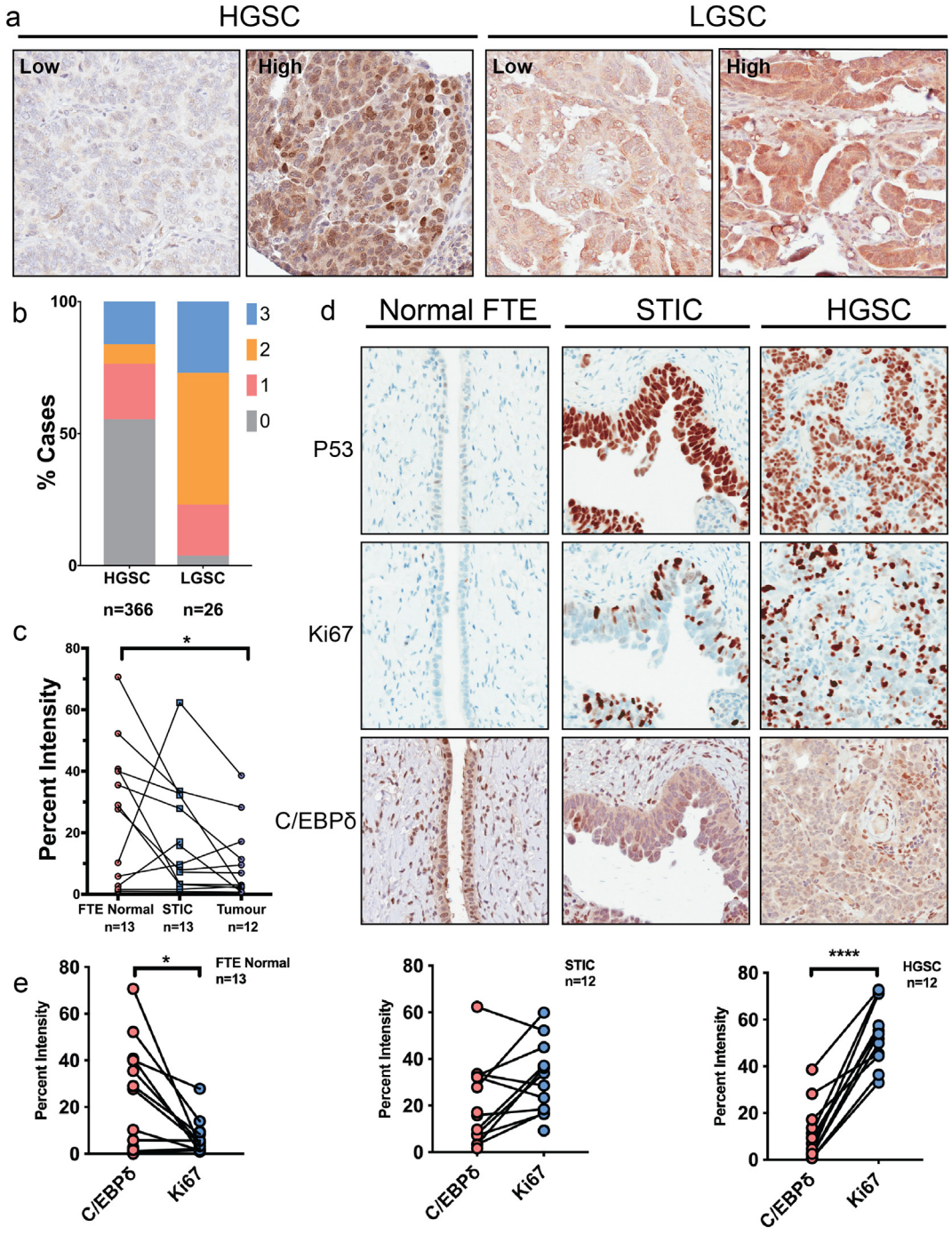

Fig. 1. C/EBPδ is differentially expressed across two distinct serous histotypes, HGSC and LGSC. a. Representative IHC nuclear staining of C/EBPδ showing examples of HGSC and LGSC expressing low and high C/EBPδ expression, respectively. Percentage of C/EBPδ staining was scored from 0 (low) to 3 (high). b. Histogram shows C/EBPδ expression levels stratified by scores across a cohort of HGSC (n = 366) and LGSC (n = 26). c. Dot plot of representative samples shows decreasing C/EBPδ IHC staining across normal FTE (n = 13), STIC (n = 13) and HGSC (n = 12). C/EBPδ expression differs significantly between normal FTE and HGSC tumour samples. d. Representative IHC staining of p53, Ki67 and C/EBPδ in histologically normal fallopian tube epithelia, STIC and HGSC, respectively. e. Quantification of both C/EBPδ and Ki67 levels in FTE (n = 13), STIC (n = 12), and HGSC cases (n = 12) demonstrated an inverse relationship between C/EBPδ and Ki67 in normal ($p = 0.01$) and HGSC cases ($p = 0.0001$). Data are represented as mean +/− SEM and *p*-values are calculated using student *t*-tests, two-tailed ($^{*}p < 0.05$; $^{****}p < 0.0001$).

expression (histoscore of +2/+3). Seventy-six per cent (76.9%, 20/26) of LGSC cases had medium to high expression compared to 23% (6/26) with low C/EBPδ expression. Overall, HGSC had 2-fold lower C/EBPδ protein expression relative to LGSC ($p = 0.0004$) (Fig. 1b).

In the TCGA ovarian cancer dataset [18], 2.5% (8/316) of HGSC cases had an amplification and 3.1% (10/316) had a shallow deletion of *C/EBPδ* with few cases (<10%) having the mRNA downregulated (http://bit.ly/2DW9QPa).

3.2. Reduced C/EBPδ expression levels in STIC lesions reflect early changes observed in HGSC

Since C/EBPδ protein levels are higher in normal FTE and differentially expressed in HGSC, we assessed C/EBPδ protein expression in a small cohort of matched normal FTE, STIC and HGSC (n = 13). Our data revealed that 53.8% (7/13) of normal fallopian tube cases had higher C/EBPδ protein expression levels (+2/+3 expression) compared

to other STIC's and HGSC, whereas in 46% (6/13) of cases, C/EBPδ protein expression was maintained between FTE and STIC. In normal FTE, high C/EBPδ protein expression was associated with low proliferation as determined by Ki67 expression ($p = 0.02$). In STIC, however, C/EBPδ expression was slightly lower than in normal FTE, while Ki67 expression increased relative to normal FTE ($p = 0.08$) and HGSCs. There were fewer C/EBPδ expressing cells in HGSC relative to highly proliferative ($Ki67^+$) and p53 expressing cells ($p < 0.0001$) (Fig. 1c-e). Overall, C/EBPδ expression was inversely related to proliferation during the transition from normal FTE, to STIC and subsequently HGSC. Given the results and the known role of C/EBPδ in cell cycle control, we sought to determine whether overexpression of C/EBPδ would regulate FTE and cancer cell growth.

3.3. Overexpression of C/EBPδ decreases proliferation in premalignant fallopian tube epithelia

3.3.1. Fallopian tube epithelia

To model p53 signatures in vitro, FTE cell lines with a p53-R175H dominant negative mutation (p53DN) and human telomerase (hTERT) over-expression were generated (Fig. 2a) [8]. As expected from immunohistochemical data, proliferating p53DN FTE cell lines had low levels of endogenous C/EBPδ protein (Fig. 2b-c). A C/EBPδ gain-of-function model was generated with a lentivirus based *pCDH-CMV-GFP-PURO* expression vector, to examine its effects on proliferation of FTE cells. Three independent FTE cell lines were transfected with either empty vector (FTE-Ctrl) or C/EBPδ cDNA vector (FTE-C/EBPδ-OE) to generate stable lines (Fig. 2a-b, Supplementary Figs. S1a, b and S2a). C/EBPδ protein abundance was confirmed by immunofluorescence (localized to the nucleus) and by western blot analyses (Fig. 2b-c, Supplementary Figs. S1a and S2a). To examine the role of C/EBPδ in cell cycle regulation, cell cycle analysis and growth kinetics were performed on FTE-Ctrl and FTE-C/EBPδ-OE cell lines. Over-expressing C/EBPδ protein reduced cell growth compared to controls, as measured by population doubling (PD) over time (19-FTE-C/EBPδ-OE versus control, 7.1-fold, $p = 0.04$; 57-FTE-C/EBPδ-OE vs control, 14.9-fold, $p = 0.01$; each in triplicate) (Fig. 2d, Supplementary Fig. S2b). Cell cycle analysis by BrdU/propidium iodide incorporation and flow cytometry in FTE cells demonstrated a propensity for C/EBPδ overexpressing cells to accumulate in the G1 phase of the cell cycle compared to FTE-Ctrl cells ($p = 0.0019$) (Fig. 2e). C/EBPδ is known to interact with *CCND1* and promotes STAT3 induced G0 cell cycle arrest [47,48]. In addition, overexpression of C/EBPδ decreased anchorage independent growth of FTE cells compared to control cells (19-FTE-p53DN-hTERT, 1.97-fold, $p = 0.0009$; 57-FTE-p53DN-hTERT, 1.41-fold, $p = 0.07$) (Fig. 2f), but increased colony formation in one cell line (Supplementary Fig. S2c). Overall, the results are consistent with decreased growth rates in 2D and 3D assays. The data show that C/EBPδ overexpression is sufficient to inhibit proliferation in FTE cells likely at the G1/S phase of the cell cycle.

3.3.2. Breast and ovarian cancer cell lines

To determine C/EBPδ mRNA basal expression levels across ovarian ($n = 42$) and breast cancer ($n = 54$) cell lines, we used publically available RNA-sequencing data from Medrano et al. [49] The data uniformly showed higher C/EBPδ mRNA levels were associated with lower proliferation rates across breast and ovarian cancer cell lines (Fig. 3a-b). Pearson correlations showed an inverse correlation between C/EBPδ and MIB1 (Ki67) in ovarian cancer cell lines, but this did not reach significance ($r = -0.183$, $p = 0.244$). A pearson correlation was also performed for all breast cancer cell lines ($r = 0.2502$, $p = 0.068$). Similarly, C/EBPδ protein expression levels in chemotherapy naive HGSC tissue by western blot analyses is low, consistent with immunohistochemical data of formalin fixed tissue (Fig. 3c). To further investigate the biological consequences of C/EBPδ protein expression in cancer cell lines, we used three breast cancer cell lines (MCF7, T47D, MDA231), and three ovarian cancer cell lines (SKOV3, Kuramochi, OVSAHO). MCF7 and T47D have wildtype p53 whereas MDA231 has a p53 mutation, and SKOV3 is p53-null [50–52]. C/EBPδ is expressed in estrogen receptor positive cancer cell lines, including MCF7 (highest), T47D, and SKOV3 with no/low expression in estrogen receptor negative MDA-231 (Fig. 3d). Across Kuramochi and OVSAHO cell lines, low levels of C/EBPδ were detected (Fig. 3e). Both Kuramochi and OVSAHO expressed Vimentin and E-cadherin, although only OVSAHO expressed CK7 (Fig. 3e).

3.4. C/EBPδ expression is associated with a MET and migratory potential in FTE

Epithelial to mesenchymal transition (EMT) has a fundamental role in cancer metastasis; restoration of the mesenchymal to epithelial transition (MET) program should efficiently slow dissemination of tumour cells [53]. Epithelial cells within fallopian tube undergo morphological changes during the menstrual cycle, evident under light microscopy [54,55]. The FTE are characteristically pseudo-stratified epithelia consisting of cuboidal and columnar epithelial cells of secretory and ciliated cells. During the pre-ovulatory (follicular) phase there is an increase in proliferation [43]. At ovulation, the secretory cells reach peak activity and secrete their nutritive contents into the lumen of the tube, then reduce in height to allow ciliated cells to move secretions by the beating of their cilia. Subsequently, in the post-ovulatory (luteal) phase, both cell types reduce in height and there is partial deciliation [56]. C/EBPδ protein expression in the mouse ovary was previously reported to be mediated by the luteinizing hormone (LH) [57] and both mRNA and protein levels are higher in FTE in the luteal phase of the ovarian cycle [26]. Using a TMA of FTE ($n = 52$) [26,43] annotated with *BRCA1* mutation and ovarian cycle status, we assessed expression of both Vimentin and E-cadherin by IHC and image analysis (Fig. 4a). Concurrent TMA slides were stained for all three proteins. In general, C/EBPδ basal protein expression was low. Interestingly, in the FTE luteal cases, where C/EBPδ expression was higher, we saw a downward shift in $Vimentin^+$ expressing FTE cells (90.2% in the follicular phase to 68.5% in the luteal phase, $p = 0.33$). No significant changes in E-cadherin were observed (91.0% in follicular phase to 88.9% in luteal phase, $p = 0.51$) (Fig. 4a-b). In vitro, FTE with a p53 dominant negative mutation and hTERT retain a mesenchymal phenotype which is characterized by Vimentin protein expression as observed in FTE in vivo (Fig. 4d, Supplementary Fig. S2a). FTE overexpressing C/EBPδ showed a distinctive epithelial-like phenotype with well-defined sheets of adhering cells compared to control cells which had more elongated mesenchymal shape (Fig. 4c). Western blot analyses demonstrated a decrease in Vimentin and increase in E-cadherin protein expression in FTE overexpressing C/EBPδ compared to controls (Fig. 4d, Supplementary Fig. S2a, e). This data suggested a role for C/EBPδ in regulating cellular phenotypes and possibly cell differentiation. Overexpression of C/EBPδ in FTE significantly increased migration compared to control cells (57-FTE, 2.0-fold, $p < 0.01$, and 19-FTE, 1.6-fold, $p < 0.01$) (Fig. 4e, Supplementary Fig. S1c), but did not increase migration in one cell line (Supplementary Fig. S2d). From our results, overexpression of C/EBPδ induces a MET phenotype by suppressing Vimentin and increasing E-cadherin meanwhile decreasing cellular growth, but increasing the migratory effects of cells.

EMT genes such as *Snail*, *Twist,* and the *Zeb* family of transcription factors can change the phenotypical characteristics of cells to regulate this phenomenon. E-cadherin protein expression has been shown to be reduced in some primary ovarian carcinomas, and then re-expressed in ovarian carcinoma effusions and at metastatic sites [58]. Further, ovarian carcinoma cells can co-express E-cadherin and the EMT-associated N-cadherin suggesting that ovarian carcinoma cells undergo incomplete EMT [59,60]. We found similar co-expression of both E-cadherin and Vimentin proteins in benign FTE. Expression of E-cadherin protein goes up in neoplastic STIC lesions while the EMT associated protein, Vimentin is decreased (Supplementary Fig. S3a-b).

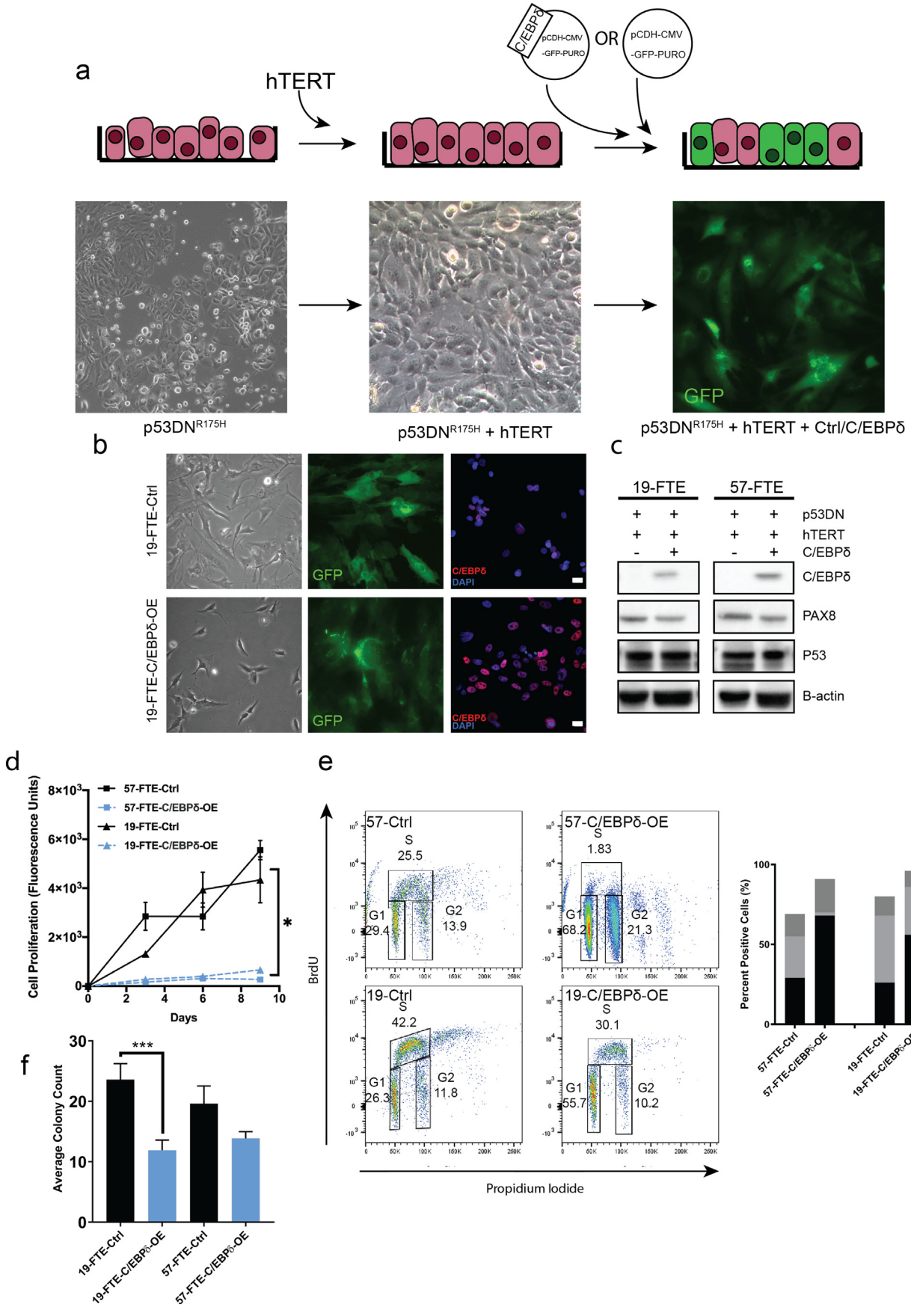
a
hTERT
C/EBPδ
pCDH-CMV -GFP-PURO
OR
pCDH-CMV -GFP-PURO
GFP
p53DN^R175H
p53DN^R175H + hTERT
p53DN^R175H + hTERT + Ctrl/C/EBPδ
b
19-FTE-Ctrl
19-FTE-C/EBPδ-OE
GFP
C/EBPδ DAPI
c
19-FTE
57-FTE
p53DN
hTERT
C/EBPδ
PAX8
P53
B-actin
d
Cell Proliferation (Fluorescence Units)
57-FTE-Ctrl
57-FTE-C/EBPδ-OE
19-FTE-Ctrl
19-FTE-C/EBPδ-OE
Days
*
e
57-Ctrl
S 25.5
G1 29.4
G2 13.9
57-C/EBPδ-OE
S 1.83
G1 68.2
G2 21.3
19-Ctrl
S 42.2
G1 26.3
G2 11.8
19-C/EBPδ-OE
S 30.1
G1 55.7
G2 10.2
BrdU
Propidium Iodide
Percent Positive Cells (%)
G2
S
G1
f
Average Colony Count
***
19-FTE-Ctrl
19-FTE-C/EBPδ-OE
57-FTE-Ctrl
57-FTE-C/EBPδ-OE

Furthermore, microarray analysis from a previous publication identified the heterogeneous expression of multiple EMT markers in normal fallopian tube epithelia across the luteal and follicular phases (Supplementary Fig. S3e). A panel of six HGSC probed for EMT/MET markers using immunoblots demonstrated the variable expression levels of these markers, consistent with other publications (Supplementary Fig. S5c). IHC analysis of a STIC and HGSC sample showed that Vimentin and E-cadherin levels were low in HGSC, but E-cadherin protein levels were higher in STIC relative to Vimentin levels (Supplementary Fig. S3c-d). Quantitative RT-PCR (qPCR) showed a significant increase in *Snail*, *Twist*, and *Zeb* in FTE-C/EBPδ-OE cells compared to FTE-Ctrl ($p < 0.01$, n = 3), in the two independent FTE cell lines (Fig. 5a). In contrast, C/EBPδ protein overexpression resulted in a decrease in protein expression levels of Twist, Slug, Zeb1, Vimentin, and N-cadherin, and an increase of Snail protein compared to control cells (Fig. 5b) indicating C/EBPδ influences a MET program in normal fallopian tube cells.

3.5. C/EBPδ induces a MET/EMT regulatory phenotype

It is well established that miRNAs regulate translation efficiency of genes by targeting mRNA [61]. This can result in differences between the amount of protein and mRNA in a cell. Certain genes, such as p53, alter the expression of miRNA which results in changes in the phenotypical characteristics of cells. Loss of p53 in mouse ovarian epithelial cells resulted in downregulation of miRNA-34b and miRNA-34c which decreased proliferation and anchorage independent growth [62]. C/EBPδ, itself has been shown to be regulated by miRNA regulatory networks with IL6 and TNF [63]. To determine whether there were differences in miRNA expression, the miRNA of FTE-C/EBPδ-OE was compared to FTE-Ctrl cells using a miRNA qPCR Array Human Ovarian cancer array (84 miRNAs). Comparisons were made between 19-FTE-C/EBPδ-OE/Ctrl and 57-FTE-C/EBPδ-OE/Ctrl cell lines (Supplementary Fig. S2f). There were 10 miRNAs that were commonly differentially expressed across both FTE-C/EBPδ over-expressing cells lines with a >2-fold change. Of these, let-7b-5p, miR-125b-1-3p, miR-143-3p, miR-145-5p, miR-224-5p and, miR-346 were up-regulated and miR-26a-5p, miR-27a-3p, miR-106-5p, miR-200b-3 were down-regulated (Fig. 5c, Supplementary Fig. S2f). miR-200b was downregulated in cells where C/EBPδ was over-expressed. MiR-200b is downregulated in ovarian cancer and has been known to target Zeb1, Zeb2, and Slug which are repressors of E-cadherin [64,65]. Low levels of miR-200 in addition to a decrease in E-cadherin results in an increase in Vimentin, N-cadherin, Twist, and Snail [66]. Overexpression of let-7b suppresses cancer cell growth [67,68] and therefore, may be one of the mechanisms by which C/EBPδ controls the fallopian tube epithelial cell cycle. C/EBPδ has also been shown to be involved in miRNA gene networks with IL6 – miR-26a-5p, TNF - miR-143-3p, and miR-27a, CREBBP – miR-27b [63]. The results suggest a role for C/EBPδ in altering miRNA expression profiles within normal FTE which influences downstream regulatory pathways of the epithelial to mesenchymal transition (Fig. 6j,k).

3.6. C/EBPδ functions as a regulatory transcriptional factor in epithelial cancer

In vitro, overexpression of C/EBPδ in SKOV3 led to an epithelial phenotype characterized by well-defined cells compared to control cells, which had a more elongated, mesenchymal phenotype (Fig. 6a, Supplementary Fig. S4a). Furthermore, FACS analysis of SKOV3 cells demonstrated an increase in $EpCAM^+$ cells and decrease in $Cd49f^+$ relative to control (Supplementary Fig. S4b). Across FTE cells, $EPCAM^+$ cell expansion was noted, consistent with the cancer cell line (Supplementary Fig. S4d). Similar to FTE, western blot analysis revealed that overexpression of C/EBPδ in SKOV3 induced E-cadherin and decreased Vimentin, Zeb1, and Zeb2 expression levels (Fig. 6b) and reduced cell growth (Fig. 6c). Interestingly, SKOV3 with C/EBPδ overexpression had reduced migration relative to control cells, which could be an effect of its p53 status (24-fold, $p < 0.001$, n = 3) (Fig. 6d). In addition, two independent ovarian cancer cell lines (Kuramochi and OVSAHO) with C/EBPδ overexpression showing a small, compact cellular phenotype relative to controls (Fig. 6e), growth was also reduced (Fig. 6f). Western Blot analysis showed increased E-cadherin and decreased Vimentin in Kuramochi and OVSAHO cells with C/EBPδ overexpression relative to controls (Fig. 6g). Kuramochi cells expressing C/EBPδ reduced the formation of anchorage independent growth colonies relative to control experiments (2.5-fold, $p = 0.02$, n = 3) but increased cell migration, however this effect was not observed in OVSAHO cells (Fig. 6h,i).

We next studied the effect of C/EBPδ overexpression in breast cancer cells lines MCF7 and T47D which have higher overall E-cadherin compared to the more mesenchymal MDA-231 cells. C/EBPδ protein expression levels are highest in MCF7, which is associated with strong expression levels of epithelial markers, E-cadherin and CK8, while MDA-231 has low C/EBPδ expression which is associated with low E-cadherin and CK8 expression and high Vimentin expression (Supplementary Fig. S6a). Since C/EBPδ basal protein expression levels were low in proliferating FTE and in HGSC, we used MCF7 cell line where basal levels of C/EBPδ can be clearly detected by western blot analysis to determine if C/EBPδ is necessary to maintain proliferation (Supplementary Fig. S6a, b). A non-targeting (NT) control cell line and a C/EBPδ-knockdown (KD) stable cell line were generated in MCF7 (Supplementary Fig. S6b). Growth inhibitory effects of C/EBPδ overexpression were observed in cancer cell lines which resulted in reduced cell growth in MCF7, T47D, but an increased growth in MDA-231 compared to controls (Supplementary Fig. S6D, H). Proliferation assays demonstrated that in MCF7, C/EBPδ overexpression decreased cell growth at day 3 (3.6-Fold, $p = 0.01$), day 5 (4.7-Fold, $p = 0.04$), day 7 (11.43-Fold, $p = 0.002$), and day 10 (30-Fold, $p = 0.002$) compared to control cells (Supplementary Fig. S6d). Loss of C/EBPδ expression in MCF7 had no significant effect on cell growth (Supplementary Fig. S6d). However, C/EBPδ protein overexpression resulted in a decrease of anchorage independent growth (1.6-fold, $p = 0.01$) (Supplementary Fig. S6F). In contrast, MDA231 with C/EBPδ overexpression resulted in increased soft agar colony formation relative to control cells (Supplementary Fig. S6i). A second breast cancer cell line, T47D, overexpressing C/EBPδ demonstrated a signifcant decrease in cell proliferation at day 3 (11.45-Fold, $p = 0.00009$), day 5 (11.67-Fold, $p = 0.01$), and day 10 (12.5-Fold, $p = 0.01$) (Supplementary Fig. S6g,h), but in the more mesenchymal cell line, MDA231, C/EBPδ increased growth rates slightly compared to controls, albeit not statistically significant ($p = 0.35$) (Supplementary Fig. S6g, h). In the context of MCF7, a hormonally responsive breast cancer cell line, C/EBPδ expression is sufficient to inhibit anoikis by anchorage independent growth.

Fig. 2. Overexpression of C/EBPδ reduces cell proliferation. a. In vitro model of C/EBPδ overexpression in premalignant fallopian tube epithelia. Fallopian tube epithelial cells have a limited life span in vitro. To generate premalignant cells, FTE were infected with lentivirus containing p53 dominant negative mutation ($p53DN^{R175H}$). Cells with $p53DN^{R175H}$ were selected and subsequently immortalized using htert. FTE-p53DN-htert cells were then infected with either control vector or C/EBPδ. b. Phase contrast microscopy images of a FTE cell line, showing control cells (19-FTE-p53DN-hTERT-Ctrl) and C/EBPδ overxpressing cells (19-FTE-p53DN-hTERT-C/EBPδ-OE) with corresponding images of GFP expression (green) as a marker of successfully infected cells, and C/EBPδ expression (red) in the nucleus (blue). c. Confirmation of C/EBPδ protein expression by western blot in two FTE cell lines, 19-FTE and 57-FTE. PAX8 is a fallopian tube epithelial marker. d. Cell growth measured as population doublings across days in two cell lines, 19-FTE and 57-FTE. C/EBPδ overexpression significantly reduced growth in premalignant FTE. e. To determine cell cycle distribution, BrdU incorporation, and DNA content were analyzed by flow cytometry (n = 3). Representative plot showing percentage distribution of cells across cell cycle control verses C/EBPδ overexpressing cells using two cell lines, 19-FTE and 57-FTE. Statistical significance was set at $p < 0.05$. C/EBPδ overexpression inhibited proliferation by accumulating cells in G1 phase of the cell cycle f. Anchorage independent growth assays (soft agar assays) performed on FTE-Ctrl and FTE-C/EBPδ-OE cells (n = 3).

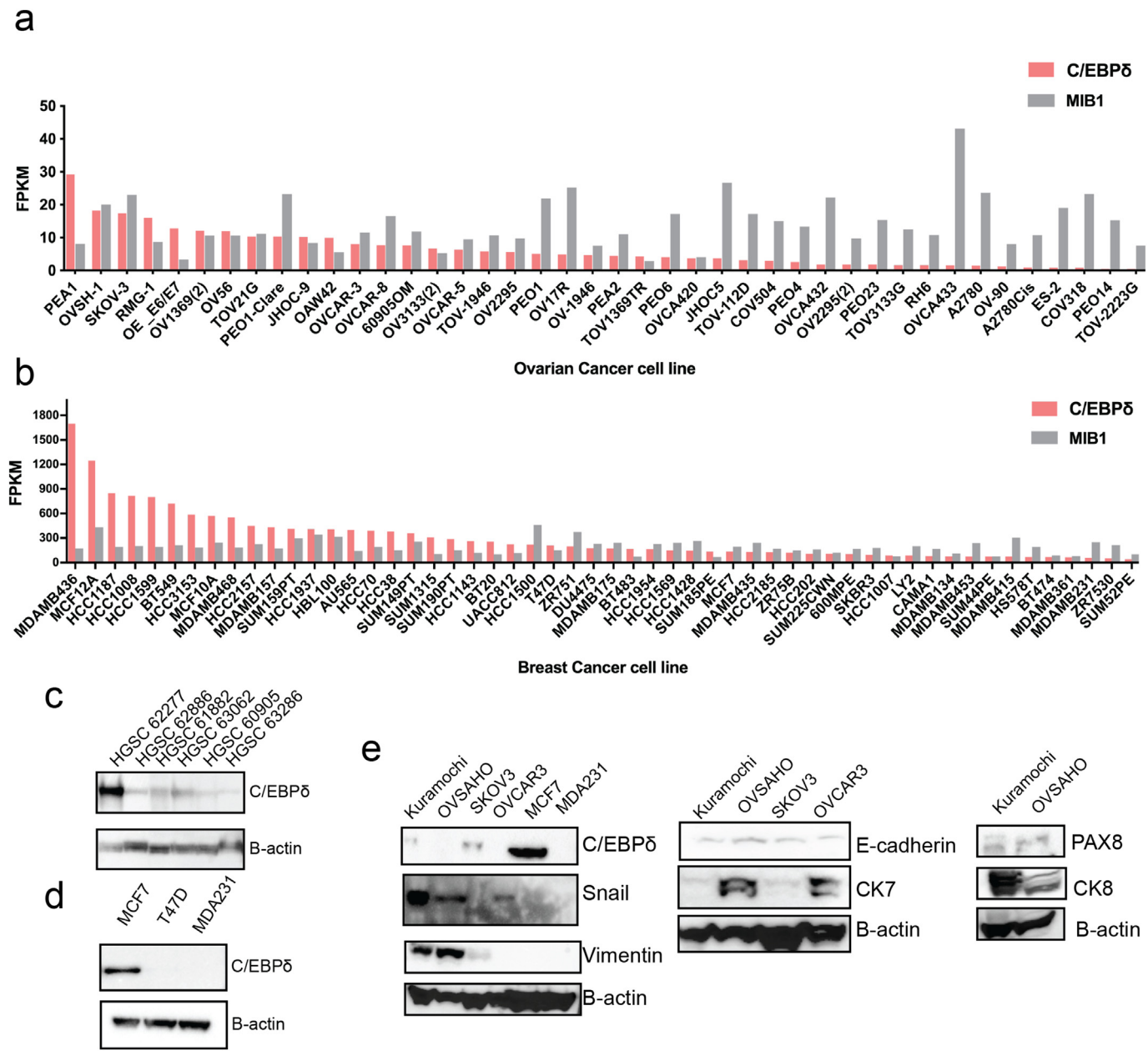

Fig. 3. C/EBPδ mRNA expression levels show an inverse correlation with proliferation marker and protein expression varies in HGSC samples. a. mRNA expression levels measured as fragment per kilobase per million reads (FPKM) of C/EBPδ and MIB1 (Ki67) across a panel of 42 ovarian cancer cell lines shows an inverse correlation between C/EBPδ and MIB1 mRNA expression levels. Pearson correlation comparing all ovarian cancer cell lines was performed. b. Similarly, C/EBPδ and MIB1 mRNA expression levels were analyzed across a panel of 54 breast cancer cell lines showing higher levels of C/EBPδ were associated with lower levels of MIB1 expression. mRNA expression levels are displayed as FPKM. A pearson correlation was performed between C/EBPδ and MIB1. c. Western blot analysis of C/EBPδ expression across six HGSC tumour samples. B-actin is used as a loading control. d. Western blot analysis of C/EBPδ expression across three breast cancer cell lines, MCF7, T47D, and MDA231. e. Western blot analysis of basal C/EBPδ protein expression, epithelial, and mesenchymal markers across several ovarian cancer cell lines.

EMT markers such as Snail and Twist were expressed in T47D cells and Zeb2 was expressed in all three cell lines (Supplementary Fig. S5a). In MCF7, overexpression of C/EBPδ resulted in an increase in E-cadherin expression while silencing of C/EBPδ reversed E-cadherin levels (Supplementary Fig. S6b). Using T47D cells overexpressing C/EBPδ there was no effect on Snail protein expression and a slight decrease in Twist protein expression (Supplementary Fig. S5b). An in-vitro observation of MCF7 cells with overexpression C/EBPδ using bright field microscopy showed cells were more compact and rounded, indicative of an epithelial phenotype, compared to cells with a C/EBPδ knockdown, which displayed filipodia and were less compact (Supplementary Fig. S6c). As in FTE, the overexpression of C/EBPδ in MCF7 cells resulted in significantly more cells migrating relative to control cells (1.74 fold, $p = 0.004$) (Supplementary Fig. S6e). Taken together, as normal cells transition toward a neoplastic state, C/EBPδ protein expression decreases resulting in less control over the cell cycle and as a consequence pushes the cell to a more epithelial phenotype (MET) which in the context of high-grade serous cancer makes it more permissive to transformation (Fig. 6j,k). In many in vitro and in vivo models of EMT, polarized epithelial cells EMT, cells lose polarity, cell-cell adhesion, and acquire migratory and invasive properties [69]. In the FTE, a polarized epithelial layer of ciliated and secretory, Cytokeratin 18 ($CK18^{+}$) cells, express both Vimentin and E-cadherin, and undergo a modified mesenchymal to epithelial transition during serous tubal intraepithelial transformation.

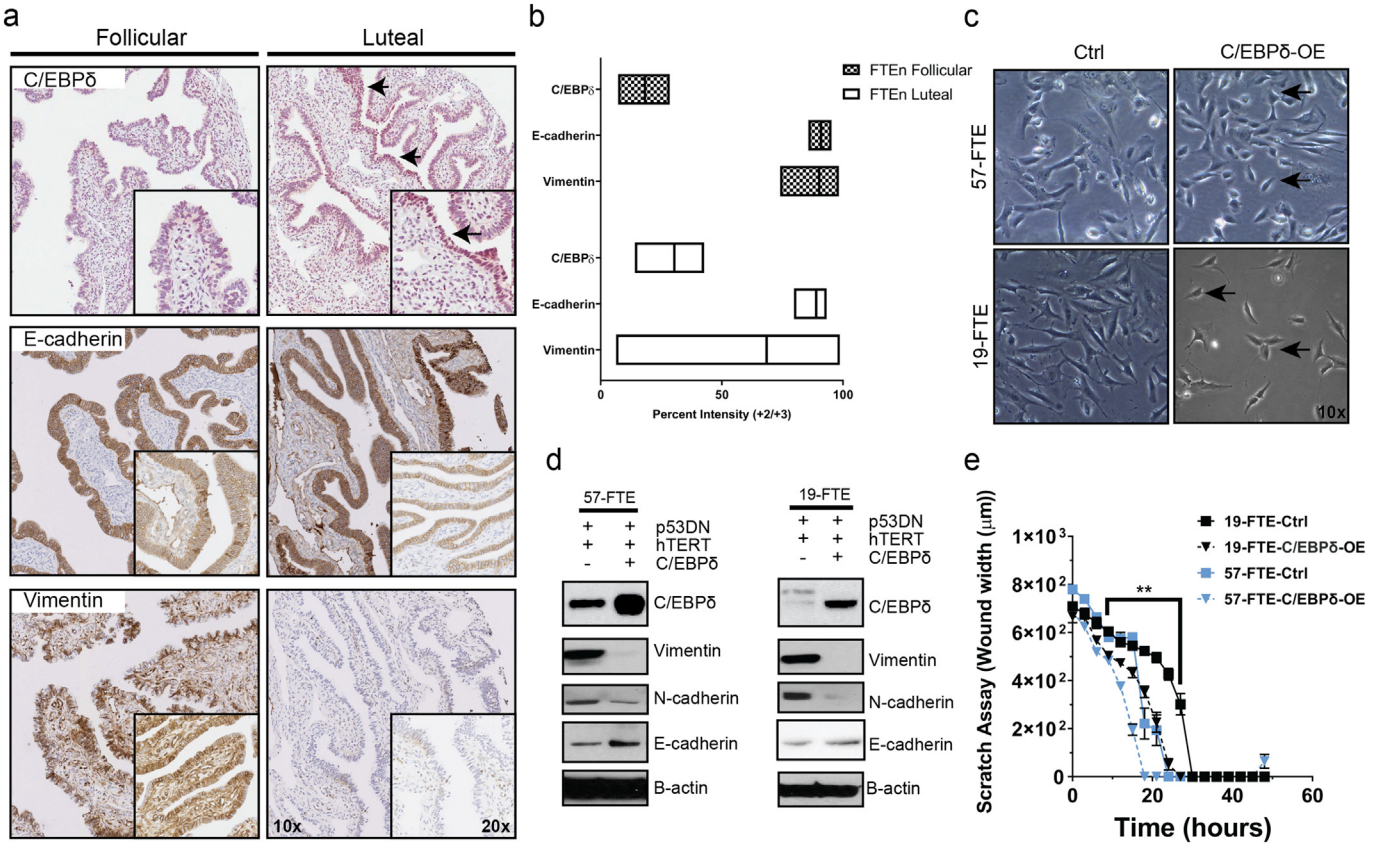

Fig. 4. CEBPD overexpression promotes an epithelial cell phenotype with migratory potential. a. Representative IHC staining of C/EBPδ, E-cadherin and Vimentin in fallopian tube epithelia from the luteal and follicular phases of the menstrual cycle. b. Quantification of C/EBPδ, E-cadherin and Vimentin protein expression in 21 fallopian tube epithelia cases. c. Macroscopic images were taken using bright field light microscopy of two FTE cell models, 57-FTE and 19-FTE showing control verses C/EBPδ overexpressing cells. Black arrows indicate elongations from filopodia in C/EBPδ overexpressing cells. Images were taken at 20× magnification. d. In vitro analysis of 57-FTE and 19-FTE using western blots showing C/EBPδ, E-cadherin, Vimentin, N-cadherin expression relative to control cells. B-actin is used as a loading control. e. A wound healing assay was performed on 57-FTE and 19-FTE cell lines to demonstrate migration potential (n = 3). Wound width (μm) was measured against time of experiment (measured in hours).

4. Discussion

In this study, we present a role for C/EBPδ in the regulation of an EMT/MET program during early preneoplastic changes in the fallopian tube. Expression of C/EBPδ is high in ~40% of STICs and expression from STIC to HGSC is maintained in the 40/60% high-low ratio. High expression of C/EBPδ promotes a partial EMT/MET phenotype in FTE cells. C/EBPδ has a role in promoting cell migration despite decreasing cell proliferation, a characteristic that has been identified in mesenchymal-like breast cancer cells expressing YB-1 [70]. It is possible that C/EBPδ reduces proliferation rates thereby decreasing cell density allowing for the monolayer migration [71]. In the context of a p53 mutation and C/EBPδ, cells become more mesenchymal relative to baseline, which results in an MET phenotype. This feature, as seen in the luteal phase of the ovarian cycle, results in slower growth. Independent of C/EBPδ, the fallopian tube epithelial cells express a mesenchymal protein, Vimentin, which changes with the ovulatory cycle. This highlights a new appreciation of the inherent epithelial and mesenchymal features of FTE cells which either facilitate or inhibit tumorigenesis (Fig. 6j,k).

Previously, by comparing hormonally driven changes of phenotypically normal FTE from women with and without a BRCA1 mutation, we identified several differentially expressed genes with known functions that promote tumour development and metastasis [26,44]. Amongst these genes, C/EBPδ, a transcriptional regulator of cellular differentiation, inflammatory signaling, hypoxia adaptation, and metastatic progression, was increased during the luteal phase of the ovarian cycle [26]. C/EBPδ has dualistic roles as a tumour suppressor or oncogene and has been called a master regulator gene. In breast cancer cell line, MCF7, C/EBPδ was shown to decrease CylinD1 by mediating CCND1 degradation through Cdc27/APC3 regulation [72,73]. In the epidermoid skin cancer cell line, A431, C/EBPδ also decreased cancer cell proliferation induced by interacting with E2F1 and Rb [35]. In leukemia, CML, KCL22 and K562 cell lines, expression of C/EBPδ was associated with downregulation of c-Myc and cyclinE1 and upregulation of the cyclin-dependent kinase inhibitor p27 [32]. We sought to establish C/EBPδ's role in the pathogenesis of high-grade serous ovarian cancer. Our tissue-based data revealed that 77% of a cohort of HGSC cases had low C/EBPδ protein expression compared to LGSCs. This difference may be reflective of the underlying pathogenic routes to these distinct tumours that arise in the fallopian tube [3,74]. HGSC is fast growing and has a high proliferative index compared to LGSC, which is slow growing and indolent [75]. In our cohort of normal FTE and serous intraepithelial carcinoma in situ (STIC) cases, C/EBPδ expression was inversely correlated to Ki67 expression. Higher expression levels of C/EBPδ were associated with lower Ki67 staining and the trend was consistent in HGSCs. This suggests that C/EBPδ is preferentially downregulated in highly proliferative tissues of the fallopian tube and cancer.

Since C/EBPδ expression is higher in the normal tissues compared to 70% of HGSC, we used an in vitro FTE model to explore the effects of C/EBPδ overexpression in p53 dominant negative mutant cells [8]. In this study, C/EBPδ overexpression decreased cellular growth resulting in accumulation of the cells in the G1/S phase of the cell cycle. This observation was extended to ovarian and breast cancer cell lines, suggesting C/EBPδ is enough to inhibit growth. Unfortunately, endogenous levels of C/EBPδ were too low to observe an additional decrease in endogenous protein levels in the modeled premalignant fallopian tube cells. However, silencing C/EBPδ in MCF7 did not affect growth, suggesting that C/EBPδ is sufficient but not necessary for proliferation.

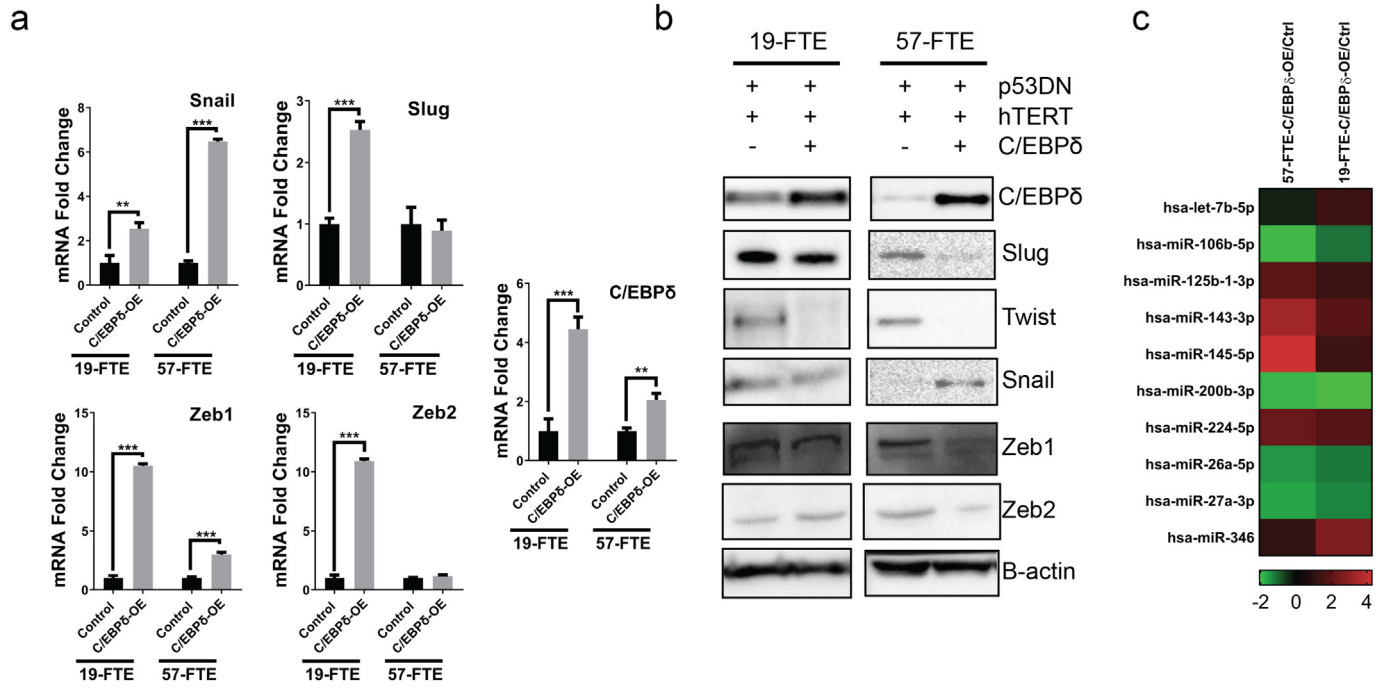

Fig. 5. C/EBPδ overexpression shows differential expression of epithelial and mesenchymal markers at the protein and mRNA level. a. A quantitative PCR (qPCR) measured the relative mRNA expression levels of C/EBPδ, and EMT/MET markers, including Snail, Slug, Zeb1, Zeb2 in two FTE cell lines overxpresing C/EBPδ verses control cells. b. A western blot analysis of EMT/MET protein markers perfomed on 57-FTE and 19-FTE overexpressing C/EBPδ compared to control cells. c. A qPCR of miRNA was performed on both 57-FTE and 19-FTE cells showing the fold change in various miRNAs in cells overexpressing C/EBPδ compared to control cells. Upregulated miRNA (Red) and downregulated (Green) were identified ($p < 0.05$, $n = 3$). Data are represented as mean +/− SEM and p-values are calculated using Student t-tests, two-tailed, and a 2-way ANOVA.

Within the normal tissue, C/EBPδ levels are higher in the luteal phase of the menstrual cycle relative to the follicular phase. The luteal phase constitutes a highly inflammatory milieu with fallopian tube epithelial cells undergoing differentiation to accommodate the motility of the ovum toward the ampulla for impregnation. C/EBPδ is rapidly induced by inflammatory signals, cytotoxic factors, and stressful conditions, which are characteristics of the luteal phase [27,76]. Given that C/EBPδ has a dichotomous role in regulating proliferation and differentiation [32], we hypothesized the expression of C/EBPδ might be slowing the growth of cells to prepare them for a transitional state. Indeed, we describe C/EBPδ's role for the first time in mediating an EMT/MET switch thereby providing FTE with epithelial plasticity and enabling the migratory potential of these cells. We hypothesize higher levels of C/EBPδ in premalignant FTE might alter cell phenotype toward an epithelial fate with potential to migrate to the ovarian surface epithelium.

One of the main points of debate regarding the fallopian tube epithelial origin of HGSC is how mesenchymal cells of origin (i.e. fallopian tube epithelial cells) form serous epithelial ovarian carcinoma. Factors other than location and proximity contribute to seeding to the ovary by fallopian tube precursor lesions. We hypothesized menstrual cycle associated genes with dual role of controlling proliferation and differentiation might play an important role in this process. In our FTE cell culture model, a p53 dominant negative (R175H) mutation was introduced to recapitulate one of the earliest known events in HGSC, namely, the p53 signature. Loss of p53 was previously shown to induce mesenchymal-like features in normal mammary epithelial cells [64]. We report similar findings in FTE. We also observed expression of Twist, Slug, Zeb1, and Zeb2 at the protein level in p53 deficient FTE cells, a feature consistent with a mesenchymal phenotype [77].

Here we showed C/EBPδ overexpression induced a partial MET, characterized by an increase in expression of epithelial markers, E-cadherin and CK7, and a decrease in expression of mesenchymal markers, including Vimentin and N-cadherin. This was observed in FTE precursor lesions as well as cancer cell lines. Furthermore, upon C/EBPδ overexpression, a decrease in the expression of Twist, Slug, and Zeb1 were observed at the protein level. The data suggests a role for C/EBPδ in regressing the mesenchymal phenotype of p53 mutated FTE cells. The overexpression of C/EBPδ still increased the migratory rate of FTE cells and cancer cell lines. However, knocking down C/EBPδ in a cancer cell line did not demonstrate a significant difference in migration relative to controls. In urothelial cancers (UC), C/EBPδ enhanced the invasiveness of UC cells through direct binding and upregulation of MMP2 [78]. This highlights a dichotomous role of C/EBPδ as a tumour suppressor or oncogene with tumour promoting potentials depending on the tissue and the genomic context within which the gene is expressed. Primary fallopian tube cells have limited growth expansions in vitro [8] and therefore, conducting these experiments in the p53 wild type setting was not feasible. However, the presence of p53-R175H mutation along with C/EBPδ over-expression promotes cellular migration.

Human fallopian tube epithelial cells do not require intravasation to metastasize to the ovary and other organs in the abdominal cavity. FTE cells are exposed to the peritoneal cavity where they can slough off easily and disseminate to other locations. This study highlights new roles for C/EBPδ in HGSC and separately features intriguing EMT/MET hybrid FTE phenotypes influenced by the ovulatory cycle. This hybrid-pleiotropic phenotype in cancer is implicated in cancer metastasis, cancer stem cell plasticity, chemoresistance, and immune evasion [79,80], all features also attributed to ovarian cancer biology and heterogeneity. These EMT/MET protein expressions observed in the histologically normal fallopian tube epithelia and pre-malignant lesions need further study to identify core transcriptional and genomic/epigenomic networks driving fallopian tube epithelia transformation. Further, FTE cells endogenously express well-established mesenchymal markers like Vimentin and epithelial markers as E-cadherin simultaneously which can be considered an intermediate phenotype [53]. Acquisition of mutant p53 is not required for these cells to express mesenchymal genes, but may play a role in promoting anoikis and survival in the peritoneal cavity once detached from the basement membrane. During the

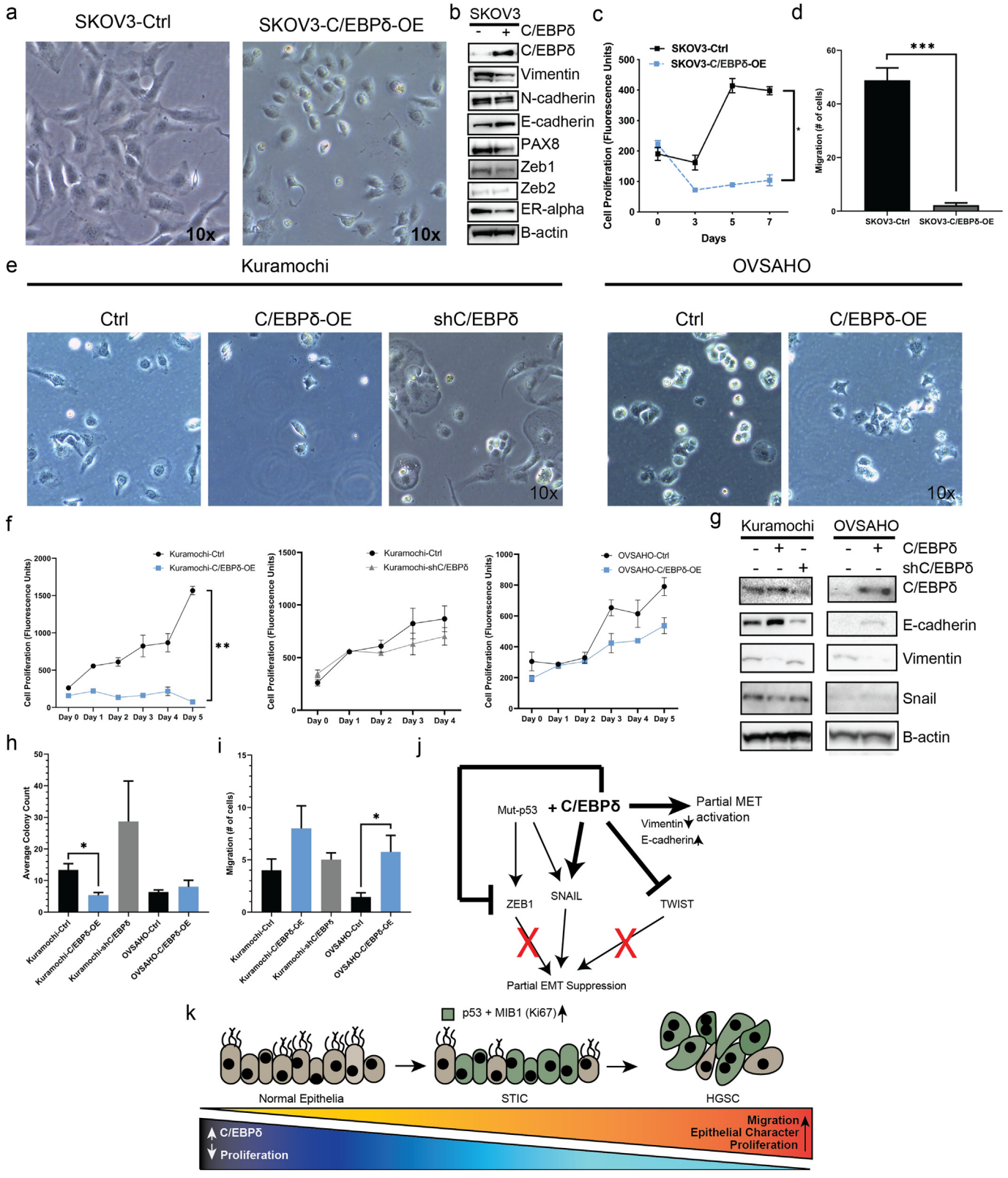

Fig. 6. C/EBPδ increases E-cadherin expression in cancer cell lines. a. Representative macroscopic images of SKOV3 cell line overexpressing C/EBPδ compared to control, taken using bright field light microscopy at 20× magnification. b. Western blot analysis of C/EBPδ, mesenchymal markers Vimentin and N-cadherin, epithelial markers E-cadherin and Pax8, EMT/MET markers, including Zeb1, Zeb2, as well as ERα in SKOV3 cells overexpressing C/EBPδ compared to controls. c. Growth curve of SKOV3 cells expressing C/EBPδ relative to control cells with no C/EBPδ. d. Migration assay of SKOV3 cells with C/EBPδ-OE relative to control cells. e. Bright Field microscopy images of Kuramochi and OVSAHO expressing C/EBPδ show differences in cellular phenotype at 10× magnification. f. Cell proliferation assays of Kuramochi and OVSAHO with C/EBPδ-OE measured in fluorescence units ($p < 0.05$, n = 3) g. Western blot analysis showing expression of C/EBPδ, E-cadherin, and Vimentin. h. Soft agar colony assay performed on Kuramochi and OVSAHO cells show a decrease in colony formation of Kuramochi cells expressing C/EBPδ (n = 3). i. A transwell migration assay shows increased migration in Kuramochi and OVSAHO cells expressing C/EBPδ (n = 3). j. A proposed pathway demonstrating the role of C/EBPδ in the EMT/MET in the context of fallopian tube epithelia. k. A model showing the role of C/EBPδ in the development of HGSC. Data are represented as mean +/− SEM and p-values are calculated using unpaired t-tests, two-tailed (*$p < 0.05$; *** $p < 0.001$).

ovulatory cycle, C/EBPδ decreases cell growth and can influence mesenchymal gene expression potentially through miRNAs. Although the connection between C/EBPδ and miRNA requires further study, several publications have highlighted the role of C/EBPδ in regulating miRNA resulting in downstream phenotypical differences in cells with and without C/EBPδ, as is the case of miR-193b in urothelial human carcinoma's which demonstrated and anti-tumourigenic function of C/EBPδ through miR-193b in NUTB1 human urothelial carcinoma cell line [81]. In this context, we suggest a model whereby C/EBPδ's initial expression in premalignant FTE would slow cell cycle progression and allow these cells to acquire epithelial phenotype with potential to avoid anoikis and migrate to the ovary. Once these cells have migrated to the ovary, decreased expression of C/EBPδ promotes the proliferative potential of the cells which maintain a mesenchymal phenotype reminiscent of the cell of origin. Future studies are warranted to investigate which other genes and/or gene networks promote these MET/EMT switches in early fallopian tube epithelial cells transformation and whether these networks are elicited in chemoresistant ovarian cancer.

Supplementary data to this article can be found online at https://doi.org/10.1016/j.ebiom.2019.05.002.

Acknowledgments

We thank the UHN Biobank and SCCC Biospecimen Shared Resource for sample acquisition, UHN Cancer Biobank Core Laboratory and University of Miami Confocal Core for digital imaging and image analysis services. This study was funded by the CDMRP Ovarian Cancer program (W81WH-0701-0371, W81XWH-18-1-0072), the Princess Margaret Cancer Centre Foundation, Foundation for Women's Cancer – The Belinda-Sue/Mary-Jane Walker Fund, Colleen's Dream Foundation and Sylvester Comprehensive Cancer Center. The granting agencies did not have a role in study design, data collection, data analysis, interpretation, and writing of the report.

Conflict of interest

The authors declare no competing interests.

Author contribution

Conception and design: SG, RS and PS. Development of methodology: RS, RC and SG; Acquisition of data: SG, RS, MB, LD, AM; Analysis and interpretation of data: RS, RC, BS, PS and SG; Writing, review and editing: all authors.

References

[1] Kurman RJ, Shih I-M. The dualistic model of ovarian carcinogenesis: revisited, revised, and expanded. Am J Pathol 2016;186(4):733–47.
[2] Bowtell DD, Bohm S, Ahmed AA, Aspuria PJ, Bast Jr RC, Beral V, et al. Rethinking ovarian cancer II: reducing mortality from high-grade serous ovarian cancer. Nat Rev Cancer 2015;15(11):668–79.
[3] Vang R, Shih Ie M, Kurman RJ. Fallopian tube precursors of ovarian low- and high-grade serous neoplasms. Histopathology 2013;62(1):44–58.
[4] Piek JM, Dorsman JC, Zweemer RP, Verheijen RH, van Diest PJ, Colgan TJ. Women harboring BRCA1/2 germline mutations are at risk for breast and female adnexal carcinoma. Int J Gynecol Pathol 2003;22(3):315–6 [author reply -6].
[5] Piek JMJ, van Diest PJ, Zweemer RP, Jansen JW, Poort-Keesom RJJ, Menko FH, et al. Dysplastic changes in prophylactically removed fallopian tubes of women predisposed to developing ovarian cancer. J Pathol 2001;195(4):451–6.
[6] Visvanathan K, Shaw P, May BJ, Bahadirli-Talbott A, Kaushiva A, Risch H, et al. Fallopian tube lesions in women at high risk for ovarian Cancer: a Multicenter study. Cancer Prev Res (Phila) 2018;11(11):697–706.
[7] Folkins AK, Jarboe EA, Saleemuddin A, Lee Y, Callahan MJ, Drapkin R, et al. A candidate precursor to pelvic serous cancer (p53 signature) and its prevalence in ovaries and fallopian tubes from women with BRCA mutations. Gynecol Oncol 2008;109(2):168–73.
[8] George SH, Milea A, Sowamber R, Chehade R, Tone A, Shaw PA. Loss of LKB1 and p53 synergizes to alter fallopian tube epithelial phenotype and high-grade serous tumorigenesis. Oncogene 2016;35:59–68.
[9] George SH, Shaw P. BRCA and early events in the development of serous ovarian Cancer. Front Oncol 2014;4:5.
[10] Karst AM, Levanon K, Drapkin R. Modeling high-grade serous ovarian carcinogenesis from the fallopian tube. Proc Natl Acad Sci U S A 2011;108(18):7547–52.
[11] Jazaeri AA, Bryant JL, Park H, Li H, Dahiya N, Stoler MH, et al. Molecular requirements for transformation of fallopian tube epithelial cells into serous carcinoma. Neoplasia 2011;13(10):899–911.
[12] Sehdev AS, Kurman RJ, Kuhn E, Shih Ie M. Serous tubal intraepithelial carcinoma upregulates markers associated with high-grade serous carcinomas including Rsf-1 (HBXAP), cyclin E and fatty acid synthase. Mod Pathol 2010;23(6):844–55.
[13] Visvanathan K, Vang R, Shaw P, Gross A, Soslow R, Parkash V, et al. Diagnosis of serous tubal intraepithelial carcinoma based on morphologic and immunohistochemical features: a reproducibility study. Am J Surg Pathol 2011;35(12):1766–75.
[14] Shaw PA, Rouzbahman M, Pizer ES, Pintilie M, Begley H. Candidate serous cancer precursors in fallopian tube epithelium of BRCA1/2 mutation carriers. Mod Pathol 2009;22(9):1133–8.
[15] Milea A, George SH, Matevski D, Jiang H, Madunic M, Berman HK, et al. Retinoblastoma pathway deregulatory mechanisms determine clinical outcome in high-grade serous ovarian carcinoma. Mod Pathol 2014;27:991–1001.
[16] Levanon K, Sapoznik S, Bahar-Shany K, Brand H, Shapira-Frommer R, Korach J, et al. FOXO3a loss is a frequent early event in high-grade pelvic serous carcinogenesis. Oncogene 2014;33(35):4424–32.
[17] Norquist BM, Garcia RL, Allison KH, Jokinen CH, Kernochan LE, Pizzi CC, et al. The molecular pathogenesis of hereditary ovarian carcinoma: alterations in the tubal epithelium of women with BRCA1 and BRCA2 mutations. Cancer 2010;116(22):5261–71.
[18] Cancer Genome Atlas N. Integrated genomic analyses of ovarian carcinoma. Nature 2011;474(7353):609–15.
[19] Karst AM, Jones PM, Vena N, Ligon AH, Liu JF, Hirsch MS, et al. Cyclin e1 deregulation occurs early in secretory cell transformation to promote formation of fallopian tube-derived high-grade serous ovarian cancers. Cancer Res 2014;74(4):1141–52.
[20] Karst AM, Levanon K, Duraisamy S, Liu JF, Hirsch MS, Hecht JL, et al. Stathmin 1, a marker of PI3K pathway activation and regulator of microtubule dynamics, is expressed in early pelvic serous carcinomas. Gynecol Oncol 2011;123(1):5–12.
[21] Kuhn E, Meeker AK, Visvanathan K, Gross AL, Wang TL, Kurman RJ, et al. Telomere length in different histologic types of ovarian carcinoma with emphasis on clear cell carcinoma. Mod Pathol 2011;24(8):1139–45.
[22] Bevers TB, Ward JH, Arun BK, Colditz GA, Cowan KH, Daly MB, et al. Breast Cancer risk reduction, version 2.2015. J Natl Compr Canc Netw 2015;13(7):880–915.
[23] Wu R-C, Wang P, Lin S-F, Zhang M, Song Q, Chu T, et al. Genomic landscape and evolutionary trajectories of ovarian cancer precursor lesions. J Pathol 2018;0(0).
[24] Lengyel E. Ovarian cancer development and metastasis. Am J Pathol 2010;177(3):1053–64.
[25] Sodek KL, Murphy KJ, Brown TJ, Ringuette MJ. Cell-cell and cell-matrix dynamics in intraperitoneal cancer metastasis. Cancer Metastasis Rev 2012;31(1–2):397–414.
[26] George SH, Greenaway J, Milea A, Clary V, Shaw S, Sharma M, et al. Identification of abrogated pathways in fallopian tube epithelium from BRCA1 mutation carriers. J Pathol 2011;225(1):106–17.
[27] Ramji DP, Foka P. CCAAT/enhancer-binding proteins: structure, function and regulation. Biochem J 2002;365(Pt 3):561–75.
[28] Balamurugan K, Sterneck E. The many faces of C/EBPδ and their relevance for inflammation and Cancer. Int J Biol Sci 2013;9(9):917–33.
[29] Wu S-R, Li C-F, Hung L-Y, Huang AM, Tseng JT, Tsou J-H, et al. CCAAT/enhancer-binding protein δ mediates tumor necrosis factor α-induced Aurora kinase C transcription and promotes genomic instability. J Biol Chem 2011;286(33):28662–70.
[30] Carro MS, Lim WK, Alvarez MJ, Bollo RJ, Zhao X, Snyder EY, et al. The transcriptional network for mesenchymal transformation of brain tumours. Nature 2010;463(7279):318–25.
[31] Cooper LAD, Gutman DA, Chisolm C, Appin C, Kong J, Rong Y, et al. The tumor microenvironment strongly impacts master transcriptional regulators and gene expression class of Glioblastoma. Am J Pathol 2012;180(5):2108–19.
[32] Gery S, Tanosaki S, Hofmann W-K, Koppel A, Koeffler HP. C/EBPδ expression in a BCR-ABL-positive cell line induces growth arrest and myeloid differentiation. Oncogene 2005;24:1589.
[33] Sanford DC, DeWille JW. C/EBPdelta is a downstream mediator of IL-6 induced growth inhibition of prostate cancer cells. Prostate 2005;63.
[34] Hutt JA, DeWille JW. Oncostatin M induces growth arrest of mammary epithelium via a CCAAT/enhancer-binding protein delta-dependent pathway. Mol Cancer Ther 2002;1.
[35] Pan Y-C, Li C-F, Ko C-Y, Pan M-H, Chen P-J, Tseng JT, et al. CEBPD reverses RB/E2F1-mediated gene repression and participates in HMDB-induced apoptosis of cancer cells. Clin Cancer Res 2010 Dec 1;16(23):5770–80. https://doi.org/10.1158/1078-0432.CCR-10-1025 Epub 2010 Oct 22.
[36] Ko C-Y, Hsu H-C, Shen M-R, Chang W-C, Wang J-M. Epigenetic silencing of CCAAT/enhancer-binding protein δ activity by YY1/Polycomb group/DNA Methyltransferase complex. J Biol Chem 2008;283(45):30919–32.
[37] Tang D, Sivko GS, DeWille JW. Promoter methylation reduces C/EBPδ (CEBPD) gene expression in the SUM-52PE human breast cancer cell line and in primary breast tumors. Breast Cancer Res Treat 2006;95(2):161–70.
[38] Takayuki Ikezoe SG, Yin Dong, O'Kelly James, Binderup Lise, Lemp Nathan, Taguchi Hirokuni, et al. CCAAT/enhancer-binding protein δ: a molecular target of 1,25-Dihydroxyvitamin D3 in androgen-responsive prostate Cancer LNCaP cells. Cancer Res 2005;65(11):4762–8.
[39] Kuppusamy Balamurugan SS, Klarmann Kimberly D, Zhang Youhong, Coppola Vincenzo, Summers Glenn H, Roger Thierry, et al. FBXW7α attenuates inflammatory signalling by downregulating C/EBPδ and its target gene Tlr4. Nat Commun 2013;4(1662):1–12.

[40] Gigliotti AP, Johnson PF, Sterneck E, DeWille JW. Nulliparous CCAAT/enhancer binding protein delta (C/EBPdelta) knockout mice exhibit mammary gland ductal hyperlasia. Exp Biol Med 2003;228.
[41] Thangaraju M, Rudelius M, Bierie B, Raffeld M, Sharan S, Hennighausen L, et al. C/EBPdelta is a crucial regulator of pro-apoptotic gene expression during mammary gland involution. Development 2005;132(21):4675–85.
[42] May T, Virtanen C, Sharma M, Milea A, Begley H, Rosen B, et al. Low malignant potential tumors with micropapillary features are molecularly similar to low-grade serous carcinoma of the ovary. Gynecol Oncol 2010;117(1):9–17.
[43] George SH, Milea A, Shaw PA. Proliferation in the normal FTE is a hallmark of the follicular phase, not BRCA mutation status. Clin Cancer Res Off J Am Assoc Cancer Res 2012;18(22):6199–207.
[44] Tone AA, Begley H, Sharma M, Murphy J, Rosen B, Brown TJ, et al. Gene expression profiles of luteal phase fallopian tube epithelium from BRCA mutation carriers resemble high-grade serous carcinoma. Clin Cancer Res 2008;14(13):4067–78.
[45] Spandidos A, Wang X, Wang H, Seed B. PrimerBank: a resource of human and mouse PCR primer pairs for gene expression detection and quantification. Nucleic Acids Res 2010;38(Database issue):D792–9.
[46] Wang X, Seed B. A PCR primer bank for quantitative gene expression analysis. Nucleic Acids Res 2003;31(24):e154.
[47] O'Rourke J, Yuan R, DeWille J. CCAAT/enhancer-binding protein-delta (C/EBP-delta) is induced in growth-arrested mouse mammary epithelial cells. J Biol Chem 1999:272.
[48] Hutt JA, O'Rourke JP, DeWille J. Signal transducer and activator of transcription 3 activates CCAAT enhancer-binding protein delta gene transcription in G0 growth-arrested mouse mammary epithelial cells and in involuting mouse mammary gland. J Biol Chem 2000;275.
[49] Medrano M, Communal L, Brown KR, Iwanicki M, Normand J, Paterson J, et al. Interrogation of functional cell-surface markers identifies CD151 dependency in high-grade serous ovarian Cancer. Cell Rep 2017;18(10):2343–58.
[50] Connor PM, Jackman J, Bae I, Myers TG, Fan S, Mutoh M, et al. Characterization of the & tumor suppressor pathway in cell lines of the National Cancer Institute anticancer drug screen and correlations with the growth-inhibitory potency of 123 anticancer agents. Cancer Res 1997;57(19):4285.
[51] Ince TA, Sousa AD, Jones MA, Harrell JC, Agoston ES, Krohn M, et al. Characterization of twenty-five ovarian tumour cell lines that phenocopy primary tumours. Nat Commun 2015;6:7419.
[52] Lee J-G, Ahn J-H, Jin Kim T, Ho Lee J, Choi J-H. Mutant p53 promotes ovarian cancer cell adhesion to mesothelial cells via integrin β4 and Akt signals. Sci Rep 2015;5:12642.
[53] Nieto MA, Huang Ruby Y-J, Jackson Rebecca A, Thiery Jean P. EMT: 2016. Cell 2016;166(1):21–45.
[54] Donnez J, Casanas-Roux F, Caprasse J, Ferin J, Thomas K. Cyclic changes in ciliation, cell height, and mitotic activity in human tubal epithelium during reproductive life. Fertil Steril 1985;43(4):554–9.
[55] Julie Crow NNA, Lewin Jackie, Shaw Robert W. Physiology: morphology and ultrastructure of fallopian tube epithelium at different stages of the menstrual cycle and menopause. Hum Reprod 1994;9(12):2224–33.
[56] Patek E, Nilsson L, Johannisson E. Scanning Electron microscopic study of the human fallopian tube. Report II. Fetal life, reproductive life, and Postmenopause. Fertil Steril 1972;23(10):719–33 **Supported by Swedish Medical Research Council Grant B72-12x-2712-04, Karolinska Institute, Stockholm, the Swedish International Development Authority, Stockholm, the Ford Foundation, U.S.A., and JEOL Inc., Tokyo, Japan.
[57] Huang A-M, Rudelius M, Sharan S, McAllister JM, Raffeld M, Christenson LK, et al. The Cebpd (C/EBPd) gene is induced by luteinizing hormones in ovarian Theca and interstitial cells but is not essential for mouse ovary function. PLoS One 2007(12):e1334–41.
[58] Davidson B, Berner A, Nesland JM, Risberg B, Berner HS, Tropè CG, et al. E-cadherin and α-, β-, and γ-catenin protein expression is up-regulated in ovarian carcinoma cells in serous effusions. J Pathol 2000;192(4):460–9.
[59] ElMoneim HMA, Zaghloul NM. Expression of E-cadherin, N-cadherin and snail and their correlation with clinicopathological variants: an immunohistochemical study of 132 invasive ductal breast carcinomas in Egypt. Clinics (Sao Paulo) 2011;66(10):1765–71.
[60] Davidson B, Tropé CG, Reich R. Epithelial-mesenchymal transition in ovarian carcinoma. Front Oncol 2012;2:33.
[61] Trobaugh DW, Klimstra WB. MicroRNA regulation of RNA virus replication and pathogenesis. Trends Mol Med 2017;23(1):80–93.
[62] Corney DC, Flesken-Nikitin A, Godwin AK, Wang W, Nikitin AY. MicroRNA-34b and MicroRNA-34c are targets of p53 and cooperate in control of cell proliferation and adhesion-independent growth. Cancer Res 2007;67(18):8433.
[63] Anandaram H, Anand DA. Computational analysis of micro RNAs compatibility in pharmacogenomic based regulatory networks of psoriatic arthritis: an initiation towards identifying a potential miRNA to treat psoriatic arthritis. Biocatal Agric Biotechnol 2018;16:545–7.
[64] Chang C-J, Chao C-H, Xia W, Yang J-Y, Xiong Y, Li C-W, et al. p53 regulates epithelial-mesenchymal transition and stem cell properties through modulating miRNAs. Nat Cell Biol 2011;13:317–+.
[65] Li Y, VandenBoom TG, Kong D, Wang Z, Ali S, Philip PA, et al. Up-regulation of miR-200 and let-7 by natural agents leads to the reversal of epithelial-mesenchymal transition in gemcitabine-resistant pancreatic cancer cells. Cancer Res 2009;69(16):6704–12.
[66] Bilyk O, Coatham M, Jewer M, Postovit L-M. Epithelial-to-Mesenchymal transition in the female reproductive tract: from Normal functioning to disease pathology. Front Oncol 2017;7:145.
[67] Xu H, Liu C, Zhang Y, Guo X, Liu Z, Luo Z, et al. Let-7b-5p regulates proliferation and apoptosis in multiple myeloma by targeting IGF1R. Acta Biochim Biophys Sin (Shanghai) 2014;46(11):965–72.
[68] Yu J, Feng J, Zhi X, Tang J, Li Z, Xu Y, et al. Let-7b inhibits cell proliferation, migration, and invasion through targeting Cthrc1 in gastric cancer. Tumour Biol 2015;36(5):3221–9.
[69] Kalluri R, Weinberg RA. The basics of epithelial-mesenchymal transition. J Clin Invest 2009;119(6):1420–8.
[70] Tognon C, Ng T, Sorensen PHB. Reduced proliferation and enhanced migration: two sides of the same coin? Molecular mechanisms of metastatic progression by YB-1 AU - Evdokimova. Valentina Cell Cycle 2009;8(18):2901–6.
[71] Tlili S, Gauquelin E, Li B, Cardoso O, Ladoux B, Delanoë-Ayari H, et al. Collective cell migration without proliferation: density determines cell velocity and wave velocity. R Soc Open Sci 2018;5(5):172421.
[72] Ikezoe T, Gery S, Yin D, O'Kelly J, Binderup L, Lemp N, et al. CCAAT/enhancer-binding protein delta: a molecular target of 1,25-dihydroxyvitamin D3 in androgen-responsive prostate cancer LNCaP cells. Cancer Res 2005;65.
[73] Pawar SA, Sarkar TR, Balamurugan K, Sharan S, Wang J, Zhang Y, et al. C/EBP{delta} targets cyclin D1 for proteasome-mediated degradation via induction of CDC27/APC3 expression. Proc Natl Acad Sci U S A 2010;107(20):9210–5.
[74] Nik NN, Vang R, Shih Ie M, Kurman RJ. Origin and pathogenesis of pelvic (ovarian, tubal, and primary peritoneal) serous carcinoma. Annu Rev Pathol 2014;9:27–45.
[75] Vang R, Shih Ie M, Kurman RJ. Ovarian low-grade and high-grade serous carcinoma: pathogenesis, clinicopathologic and molecular biologic features, and diagnostic problems. Adv Anat Pathol 2009;16(5):267–82.
[76] Yamaguchi J, Tanaka T, Eto N, Nangaku M. Inflammation and hypoxia linked to renal injury by CCAAT/enhancer-binding protein δ. Kidney Int 2015;88(2):262–75.
[77] Kogan-Sakin I, Tabach Y, Buganim Y, Molchadsky A, Solomon H, Madar S, et al. Mutant p53(R175H) upregulates Twist1 expression and promotes epithelial–mesenchymal transition in immortalized prostate cells. Cell Death Differ 2011;18(2):271–81.
[78] Wang Y-H, Wu W-J, Wang W-J, Huang H-Y, Li W-M, Yeh B-W, et al. CEBPD amplification and overexpression in urothelial carcinoma: a driver of tumor metastasis indicating adverse prognosis. Oncotarget 2015;6(31):31069–84.
[79] Mittal V. Epithelial Mesenchymal transition in tumor metastasis. Annu Rev Pathol Mech Dis 2018;13(1):395–412.
[80] Title AC, Hong S-J, Pires ND, Hasenöhrl L, Godbersen S, Stokar-Regenscheit N, et al. Genetic dissection of the miR-200–Zeb1 axis reveals its importance in tumor differentiation and invasion. Nat Commun 2018;9(1):4671.
[81] Lin S-R, Yeh H-C, Wang W-J, Ke H-L, Lin H-H, Hsu W-C, et al. MiR-193b mediates CEBPD-induced Cisplatin sensitization through targeting ETS1 and Cyclin D1 in human Urothelial carcinoma cells. J Cell Biochem 2017;118(6):1563–73.